Geochemistry, Mineralogy, and Geochronology of the U.S. Virgin Islands

U.S. GEOLOGICAL SURVEY BULLETIN 2057

AVAILABILITY OF BOOKS AND MAPS OF THE U.S. GEOLOGICAL SURVEY

Instructions on ordering publications of the U.S. Geological Survey, along with prices of the last offerings, are given in the current-year issues of the monthly catalog "New Publications of the U.S. Geological Survey." Prices of available U.S. Geological Survey publications released prior to the current year are listed in the most recent annual "Price and Availability List." Publications that may be listed in various U.S. Geological Survey catalogs (**see back inside cover**) but not listed in the most recent annual "Price and Availability List" may no longer be available.

Reports released through the NTIS may be obtained by writing to the National Technical Information Service, U.S. Department of Commerce, Springfield, VA 22161; please include NTIS report number with inquiry.

Order U.S. Geological Survey publications **by mail** or **over the counter** from the offices listed below.

BY MAIL

Books

Professional Papers, Bulletins, Water-Supply Papers, Techniques of Water-Resources Investigations, Circulars, publications of general interest (such as leaflets, pamphlets, booklets), single copies of Earthquakes & Volcanoes, Preliminary Determination of Epicenters, and some miscellaneous reports, including some of the foregoing series that have gone out of print at the Superintendent of Documents, are obtainable by mail from

U.S. Geological Survey, Map Distribution
Box 25286, MS 306, Federal Center
Denver, CO 80225

Subscriptions to periodicals (Earthquakes & Volcanoes and Preliminary Determination of Epicenters) can be obtained ONLY from the

Superintendent of Documents
Government Printing Office
Washington, DC 20402

(Check or money order must be payable to Superintendent of Documents.)

Maps

For maps, address mail orders to

U. S. Geological Survey, Map Distribution
Box 25286, Bldg. 810, Federal Center
Denver, CO 80225

Residents of Alaska may order maps from

U.S. Geological Survey, Earth Science Information Center
101 Twelfth Ave., Box 12
Fairbanks, AK 99701

OVER THE COUNTER

Books and Maps

Books and maps of the U.S. Geological Survey are available over the counter at the following U.S. Geological Survey offices, all of which are authorized agents of the Superintendent of Documents.

- **ANCHORAGE, Alaska**–Rm. 101, 4230 University Dr.
- **LAKEWOOD, Colorado**–Federal Center, Bldg. 810
- **MENLO PARK, California**–Bldg. 3, Rm. 3128, 345 Middlefield Rd.
- **RESTON, Virginia**–USGS National Center, Rm. 1C402, 12201 Sunrise Valley Dr.
- **SALT LAKE CITY, Utah**–Federal Bldg., Rm. 8105, 125 South State St.
- **SPOKANE, Washington**–U.S. Post Office Bldg., Rm. 135, West 904 Riverside Ave.
- **WASHINGTON, D.C.**–Main Interior Bldg., Rm. 2650, 18th and C Sts., NW.

Maps Only

Maps may be purchased over the counter at the following U.S. Geological Survey offices:

- **FAIRBANKS, Alaska**–New Federal Bldg, 101 Twelfth Ave.
- **ROLLA, Missouri**–1400 Independence Rd.
- **STENNIS SPACE CENTER, Mississippi**–Bldg. 3101

Geochemistry, Mineralogy, and Geochronology of the U.S. Virgin Islands

By HENRY V. ALMINAS *and* EUGENE E. FOORD
U.S. Geological Survey

ROBERT E. TUCKER
U.S. Army

U.S. GEOLOGICAL SURVEY BULLETIN 2057

UNITED STATES GOVERNMENT PRINTING OFFICE, WASHINGTON : 1994

U.S. DEPARTMENT OF THE INTERIOR
BRUCE BABBITT, Secretary

U.S. GEOLOGICAL SURVEY
Gordon P. Eaton, Director

For Sale by U.S. Geological Survey, Map Distribution
Box 25286, MS 306, Federal Center
Denver, CO 80225

Library of Congress Cataloging-in-Publication Data

Alminas, Henry V., 1938–
Geochemistry, mineralogy, and geochronology of the U.S. Virgin Islands / by Henry V. Alminas and Eugene E. Foord [and] Robert E. Tucker.
p. cm. — (U.S. Geological Survey bulletin ; 2057)
Includes bibliographical references.
Supt. of Docs. no.: I 19.3:2057
1. Geochemistry—Virgin Islands of the United States. 2. Minerals—Virgin Islands of the United States. I. Foord, Eugene E. II. Tucker, Robert E. (Robert Edward), 1952– . III. Title. IV. Series.
QE75.B9 no. 2057
[QE514]
557.3 2—dc20 93–7254
[551.97297'22] CIP

CONTENTS

FIGURES

TABLES

GEOCHEMISTRY, MINERALOGY, AND GEOCHRONOLOGY OF THE U.S. VIRGIN ISLANDS

By H.V. Alminas, E.E. Foord *and* R.E. Tucker

ABSTRACT

This geochemical and mineralogic study of the U.S. Virgin Islands indicates the presence of a previously undocumented Sn-Pb and precious metals metallogenic province in the northeastern portion of the Greater Antilles Island arc. These islands consist of island-arc related Cretaceous and Tertiary volcanic and volcaniclastic rocks, carbonates, and near-surface intrusives.

The mineralized areas on the three main islands (St. Thomas, St. John, and St. Croix) are closely related to major faults and transect all rock types. They are characterized by widespread alteration (silicification and sericitization) and an identical geochemical association consisting of Au, Ag, Te, Sn, Pb, Cu, Zn, Ni, Cr, Sb, As, Bi, Mo, Cl, and Ba. This association is exceptionally chlorine-rich and is strongly deficient in W, F, and S. The mineralization probably took place in middle and late Miocene (33–20 Ma).

The base-metal mineralogy in the secondary environment within the mineralized areas is highly unusual and complex and is dominated by halides and native metals. The native metals identified include Au, Ag, Sn, Pb, Cu, Te, Bi and a Cu-Sn alloy. Several incompletely characterized Sn and Sn-Pb chlorides or oxychlorides, in addition to cotunnite (PbCl) and paratacamite ($Cu_2(OH)_3Cl$) are widespread. The rare mineral romarchite (SnO) is more widespread than cassiterite, which is usually poorly crystallized. The native metals and the chlorides/oxychlorides are generally found intergrown in a complex manner within individual grains. It is fairly clear, however, that the mineral progression in the case of tin is from Sn chloride/oxychloride to romarchite to cassiterite within the weathering environment.

Synthesis studies in which Pb- and Sn-rich saline solutions were introduced into a $CaCO_3$-rich environment at 25° C and 1 atmosphere, produced a Pb-Sn mineralogy nearly identical, both morphologically and compositionally, to that found in outcrop samples from the U.S. Virgin Islands.

The unusual mineralogy and the laboratory studies indicate that the tin-, lead-, and precious metals-rich hydrothermal solutions might have been injected into calcareous ooze in a shallow submarine environment. The immediate vicinity of hot solution introduction might have been substantially enriched in NaCl as a result of convection cells in the sea water. All metals, aside from gold, were then precipitated in the form of chlorides and some native metals. Subsequently, organic acids related to vegetation might have served as electron donors to convert some of the chlorides to native metals.

The metallogenic province seen in the U.S. Virgin Islands very probably extends into the geologically and structurally similar British Virgin Islands located immediately to the north.

GEOGRAPHIC SETTING

The U.S. Virgin Islands are part of the Greater Antilles Island arc and are located to the east and southeast of Puerto Rico (fig. 1). They consist of three major islands (St. Thomas, St. John, and St. Croix) and some 50 smaller islands that are located primarily along the coasts of St. Thomas and St. John.

St. Thomas, the northwesternmost island, is located 64 km east of Puerto Rico and has an area of approximately 91 km^2. St. John is located immediately to the east of St. Thomas and is approximately 54 km^2. St. Croix is 216 km^2 and is located some 64 km to the south of St. Thomas.

St. Thomas and St. John are characterized by mountainous topography, with very irregular coast lines and numerous small islands adjacent to the coastlines. The topography on St. Croix is more subdued, its coastlines are regular and only two small islands occur along the northeastern coast.

The climate is maritime tropical with average annual rainfall at higher elevations in the 127–152 cm range and that at lower elevations in the 51–76 cm range. No well defined wet or dry season exists. Temperatures generally average 29° C with only a 4–5° C variation through the year.

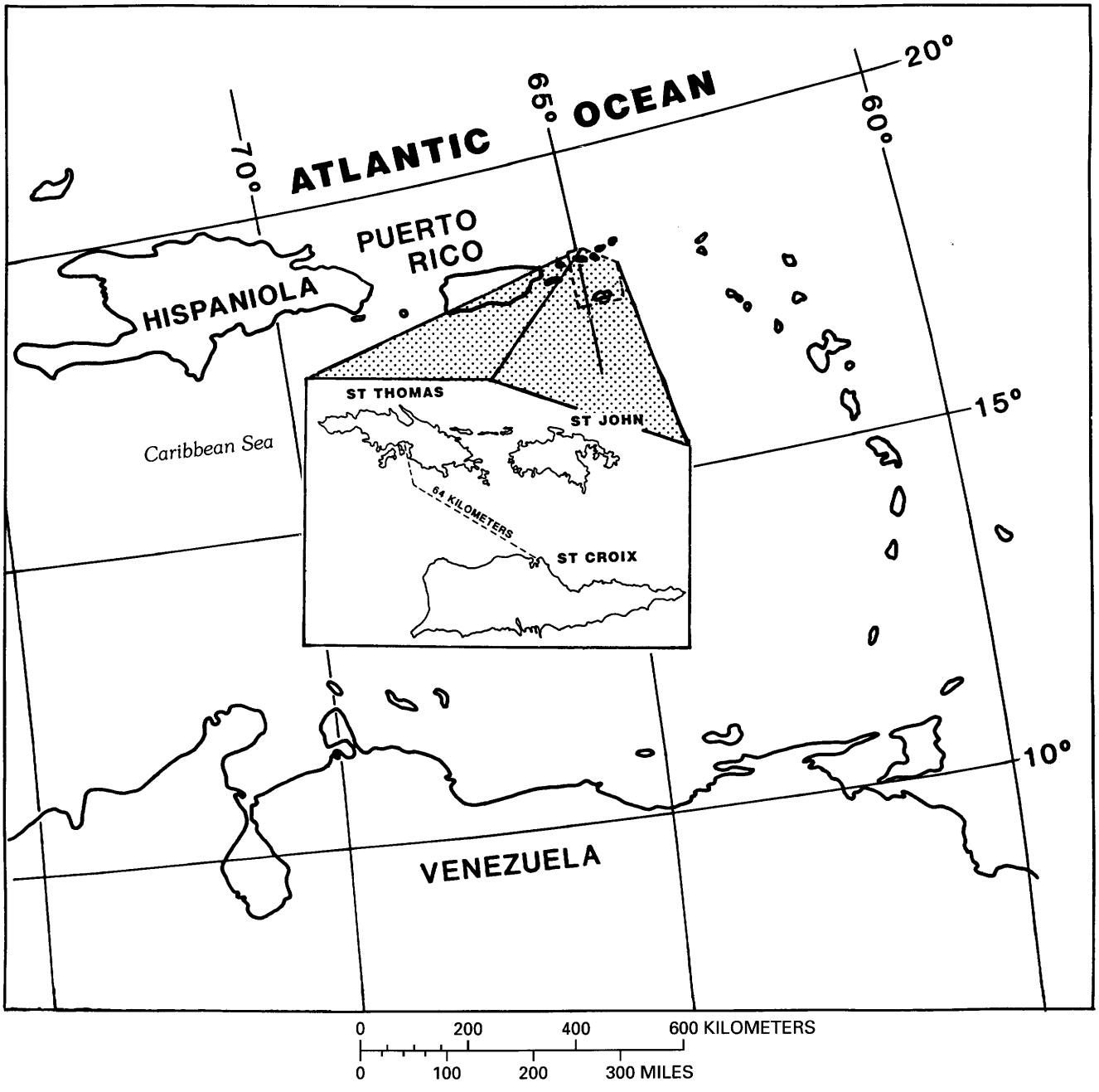

Figure 1. Regional setting of the U.S. Virgin Islands.

The streams on these islands are intermittent with generally steep gradients and short courses before emptying into the ocean.

GEOLOGY

In a regional context, the U.S. Virgin Islands are in the northeastern portion of the Greater Antilles Island arc. The Puerto Rico trench is to the north, the Annageda trench to the east and the Muertas trough to the southeast. Schell and Tarr (1978) postulated that in this northeastern corner of the Caribbean plate, the portion of the plate above the critical melting depth is carried along with the rest of the American plate beneath the edge of the Caribbean plate. The stresses exerted on the American plate, as it is bent and twisted, probably cause fracturing into segments and blocks and the reactivation of existing zones of weakness, such as oceanic fracture zones that originated near the Mid-Atlantic Ridge during initial rifting. This block-like segmentation and interaction of blocks may explain why the Puerto Rico trench appears block faulted on the surface but yields focal mechanism solutions

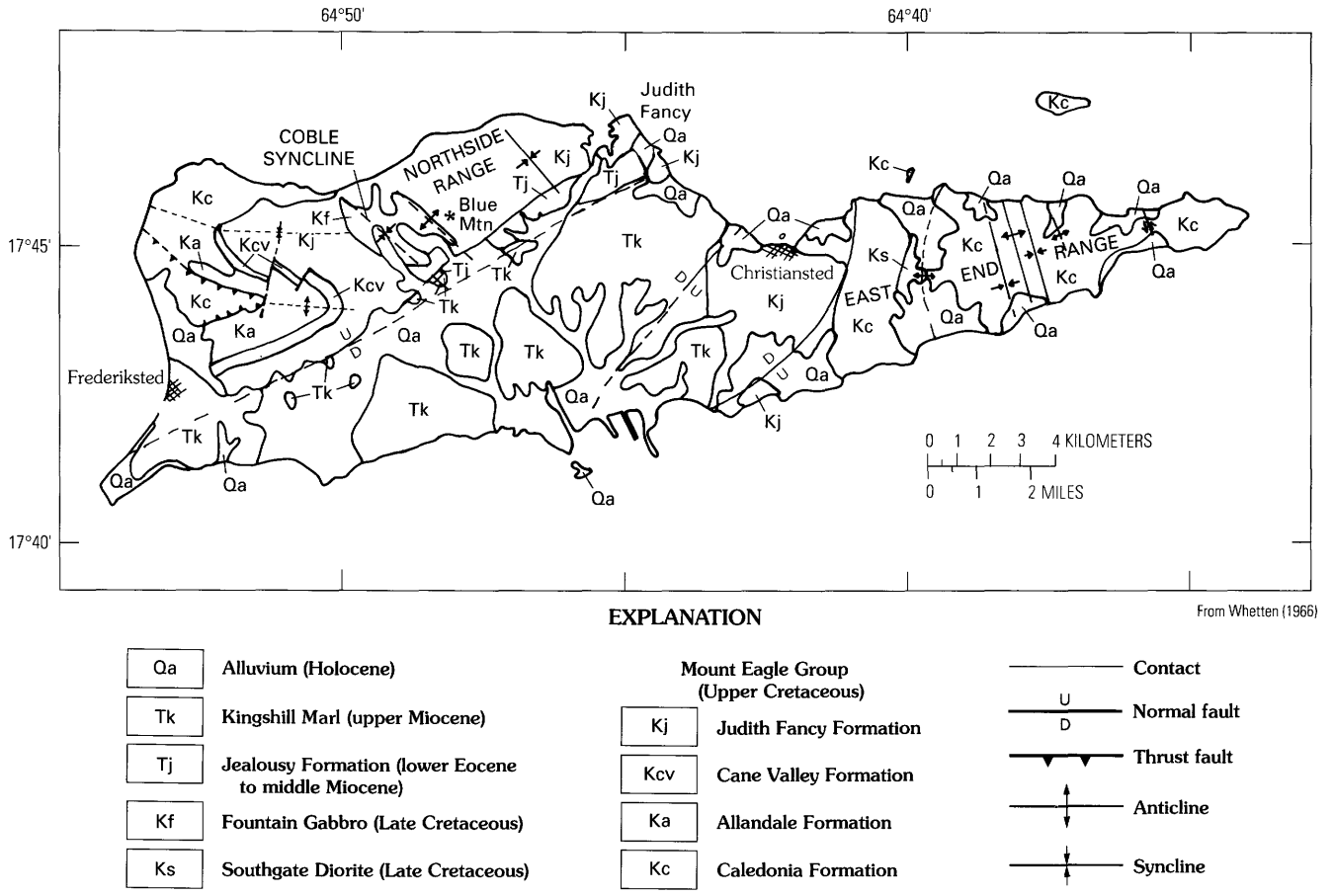

Figure 2. Simplified geologic map of St. Croix.

suggestive of horizontal thrusting and normal faulting. Further, Schell and Tarr suggested that the presence of the postulated east-to-west moving underriding slab offers a plausible explanation for such anomalous data as intermediate-depth seismicity, focal mechanism solutions, and gravity anomalies. Also, that the east-to west movement does not actively supply crustal material to the asthenosphere; thus, no volcanism occurs on the Puerto Rico–Virgin Island block.

The geology of St. Croix was mapped by J.T. Whetten in 1959–1961. A simplified geologic map of St. Croix is shown in figure 2. Whetten (1962, 1966) indicated that St. Croix is underlain by strongly folded Upper Cretaceous and gently folded Tertiary sedimentary rocks, and igneous intrusions with contact metamorphic aureoles, Late Cretaceous or early Tertiary in age.

The oldest exposed rocks on St. Croix are those of the Mount Eagle Group. The oldest formation in this group is the Caledonia Formation that is a 3,000- to 7,000-m turbidite sequence of volcanic sedimentary rocks of Campanian or older age. The Caledonia Formation grades laterally and to the south into the Allandale Formation and vertically upward into the Cane Valley Formation. The upper part of the Caledonia contains the East End Member. The Judith Fancy Formation overlies the Caledonia, Allandale, and Cane Valley Formations. All these rocks contain tuffaceous material or fragments of altered glass and of crystalline material deposited originally as volcanic ash. Whetten noted that the rocks are probably of marine origin because the sediments show signs of reworking by currents.

After deposition of the Upper Cretaceous sedimentary rocks, the region was folded and faulted and intruded by igneous rocks.

Two stocks (Fountain Gabbro and Southgate Diorite) were intruded along the axial planes of younger folds (fig. 2). The sedimentary rocks adjacent to these intrusions were contact metamorphosed to a pyroxene hornfels facies. In addition, numerous small dikes of highly variable composition occur throughout St. Croix (table 1). Lamprophyres are common in the East End Range and basaltic-andesite porphyry dikes occur in the Northside Range. Highly felsic rhyolite dikes occur at several locations (see table 1). Most of the faults on the island are normal. A graben in the center of the island is filled by approximately 2,500 m of Tertiary sedimentary rocks. Only the upper part of this is exposed. The rocks consist of montmorillonitic mudstone of the Jealousy Formation. The overlying Kingshill Marl, of late Miocene age, is a fossil coral reef. A late Miocene age is indicated for this unit by a recent study (Gill, 1990).

Table 1. X-ray fluorescence and six-step emission spectrographic analyses of olivine gabbro, gabbro, and diorite from St. Croix, U.S. Virgin Islands

[All iron expressed as Fe_2O_3. LOI, loss on ignition; N, not detected at value shown; L, detected, but below value shown]

Sample no....	1	2	5R2	14	34	36	37	42	43	44
SiO_2	49.9	43.8	51.5	45.8	53.8	53.9	47.9	45.8	44.7	58.4
Al_2O_3	20.4	16.9	19.9	18.5	15.8	17.3	14.0	14.3	13.5	17.3
Fe_2O_3	9.97	13.3	8.93	12.8	9.42	6.96	10.6	14.1	15.5	6.07
MgO	4.55	7.79	4.35	5.91	4.40	5.50	9.42	7.82	8.09	2.43
CaO	9.32	13.0	10.0	12.2	7.24	9.65	12.2	10.8	12.3	6.68
Na_2O	3.23	1.68	3.19	2.27	3.22	3.29	2.31	1.99	1.57	3.57
K_2O	0.34	0.61	0.70	0.44	1.98	1.25	0.85	0.78	0.34	1.79
TiO_2	0.65	1.08	0.57	0.81	1.03	0.39	1.04	0.88	0.98	0.52
P_2O5	0.12	1.05	0.16	0.10	0.37	0.44	0.35	0.15	0.16	0.23
MnO	0.21	0.21	0.14	0.22	0.15	0.21	0.27	0.20	0.24	0.20
LOI (900°C)	1.51	1.09	0.97	1.30	2.23	0.99	1.11	3.69	3.00	2.59
Total	100.20	100.51	100.41	100.35	99.64	99.88	100.05	100.51	100.38	99.78
B	N10	L10	10	L10	10	10	N10	N10	15	20
Ba	150	200	500	150	2,000	700	500	500	150	1,000
Co	30	50	50	30	30	50	50	70	70	15
Cr	10	200	50	50	50	200	700	500	300	20
Cu	30	300	50	30	50	30	20	70	100	30
Ga	20	30	30	30	30	30	20	30	20	30
Ni	L5	50	15	5	10	50	70	50	50	L5
Pb	15	15	15	10	15	20	15	10	10	15
Sc	20	30	30	30	20	20	30	30	50	15
Sr	700	1,000	500	300	500	700	500	500	700	700
V	200	300	150	200	200	150	200	200	300	150
Y	20	30	20	15	20	20	30	20	20	20
Zr	30	70	50	15	150	50	70	30	30	70

SAMPLE DESCRIPTIONS

1. Gabbro collected above Davis Beach at lat. 17°45'30", long. 64°50'17".
2. Olivine gabbro collected at road junction above Davis Beach at lat. 17°45'34", long. 64°49'16".

5R2. Gabbro sample collected in quarry located at lat. 17°44'19", long. 64°48'53".

14. Olivine gabbro collected in a road crust above Davis Beach at lat. 12°45'38", long. 64°49'56".
34. Gabroic diorite collected at Spring Garden at lat. 17°44'07", long. 64°41'58".
36. Gabbro collected on Marie Hill at lat. 17°44'33", long. 64°39'46".
37. Olivine gabbro collected at top of Marie Hill at lat. 17°44'37", long. 64°39'55".
42. Olivine gabbro dike collected at the Grapetree Resort at lat. 17°44'48", long. 64°36'41".
43. Olivine gabbro-gabbro dike collected at GrapetreeResort at lat. 17°44'57", long. 64°35'25".
44. Diorite dike collected at Grapetree Resort at lat. 17°44'57", long. 64°35'25".

The geology of St. Thomas and St. John has been studied by many authors including Cleve (1881), Earle (1924), Meyerhoff (1926), and more recently by Donnelly (1959, 1966). The rock unit descriptions and structural relationships of the rocks have been taken from Donnelly (1959, 1966). The rocks in the study area are island-arc related Cretaceous and Tertiary volcanic and volcaniclastic rocks, carbonates and near-surface intrusives. Simplified

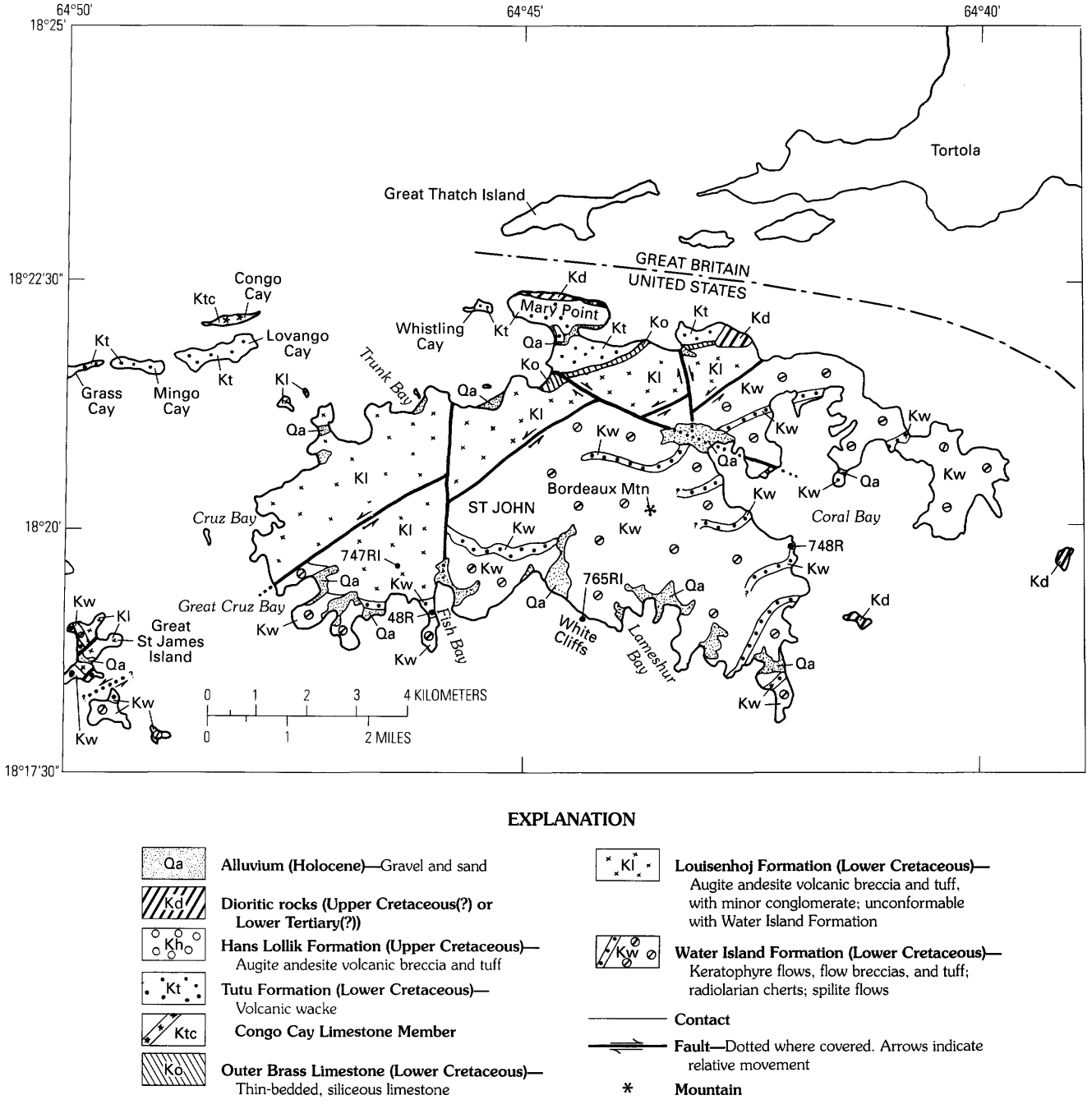

Figure 3. Simplified geologic map of St. John.

geologic maps of St. John and St. Thomas are shown in figures 3 and 4.

According to Donnelly (1959, 1966), the oldest rocks in the study area occur along the southern coasts of both islands. These rocks consist of keratophyres, spilites, and radiolarites, collectively called the Water Island Formation. The keratophyres are felsic extrusive or shallow intrusive rocks presumably of submarine origin. These rocks contain predominantly albite and quartz. The spilite is a mafic rock of submarine origin. Within the Water Island Formation the spilite is recognized by its slightly greenish outcrops. Chlorite and albite are the dominant minerals present. Remnant phenocrysts of diopside and augite are common. Amygdules are abundant and generally contain epidote, calcite, or prehnite.

Radiolarian tuffs occur predominantly near the top of the Water Island Formation and contain two genera of spumellines that resemble Thecosphaera and Flustrella

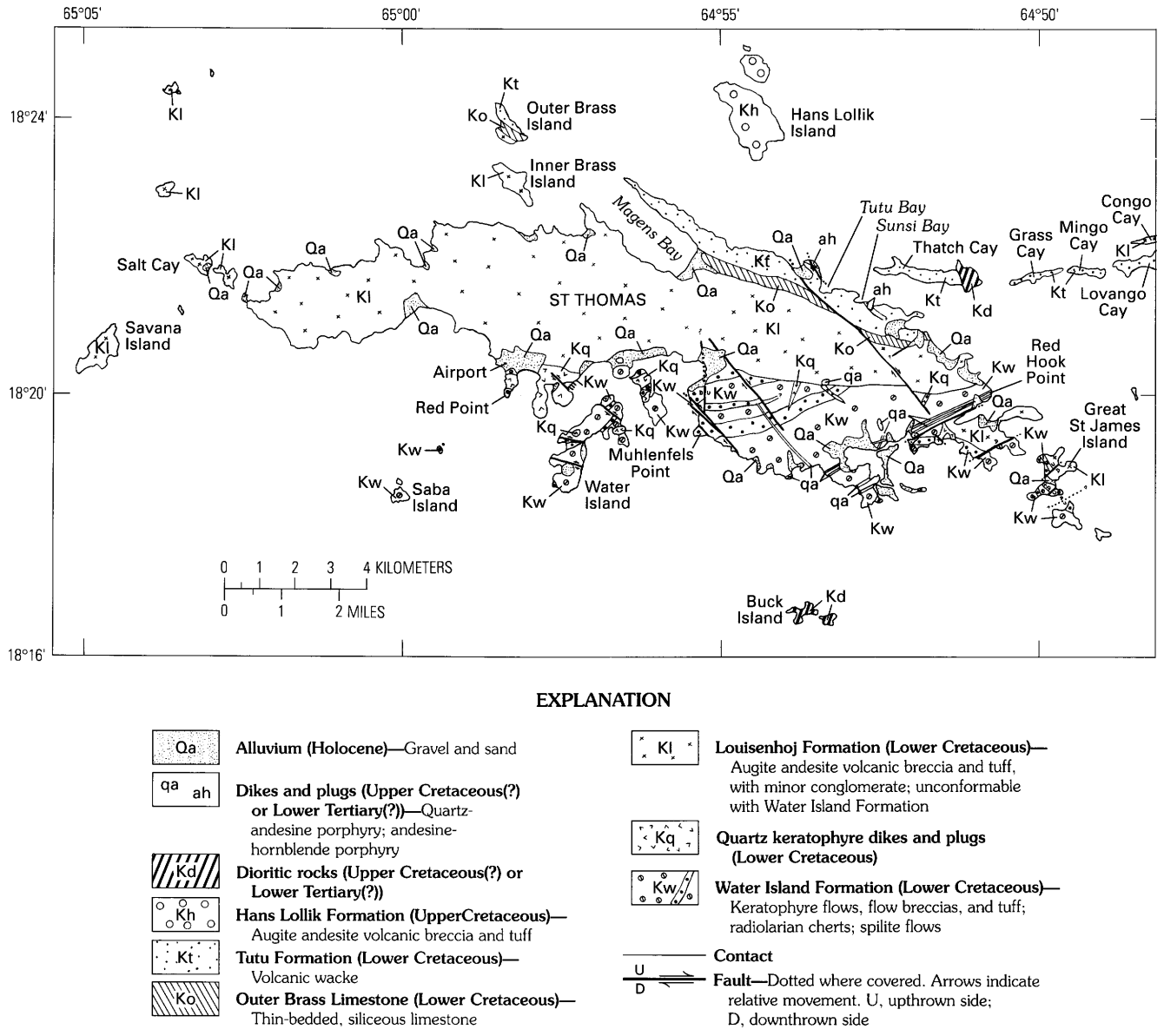

Figure 4. Simplified geologic map of St. Thomas.

similar to Early Cretaceous (144–97.5 Ma) forms in eastern Mexico (Donnelly, 1966).

The next oldest rocks are those of the Louisenhoj Formation unconformably overlying the Water Island Formation. The former unit is a sequence of pyroclastic to epiclastic augite andesites, which are believed to have originated from a nearby vent.

Overlying the Louisenhoj Formation is the Outer Brass Limestone. This unit is about 200 m thick, consisting of about 90 percent thinly bedded siliceous limestones and about 10 percent interbedded crystal tuffs. These tuffs are but a couple of meters thick.

The Tutu Formation overlies the Outer Brass Limestone. This unit consists of interbedded sequences of fine- to coarse-grained volcanic wackes that appear to be reworked Louisenhoj andesites. Some 2000 m of this unit are exposed in the American Virgin Islands. Sedimentary textures in the Tutu Formation suggest a high energy environment of deposition (Donnelly, 1966). The Tutu Formation on Grass Cay, Mingo Cay, and Lovango Cay and at Mary Point (St. John) is now a garnetiferous skarn. Within the Tutu Formation, the Coki Point Megabreccia lithofacies of Donnelly (1959) is composed of large limestone blocks up to 75 cm in length, porphyritic andesite boulders, and thin bedded wacke (Donnelly, 1966). The breccia beds are generally 10 m in thickness. The breccia crops out at Sunsi Bay and Tutu Bay on St. Thomas and possibly at Mary Point on St. John. The limestone blocks contain a neritic fauna that includes

Table 2. K-Ar age dates of rock samples from the Water Island and Louisenhoj Formations on St. Thomas and St. John Islands

[Sample number coding: ST, St. Thomas; SJ, St. John]

Sample no.	Formation	Rock type	Latitude	Longitude	Age (In megannums)
ST115R	Water Island	rhyolite	18°20'08"	64°56'39"	40.7 ± 1.1
ST120R	Water Island	rhyolite	18°19'40"	64°55'52"	65.8 ± 2.9
SJ048R	Water Island	rhyolite	18°19'39"	64°45'57"	50.2 ± 5.7
SJ685R	Louisenhoj	rhyolite	18°20'30"	64°43'27"	37.7 ± 1.1
SJ747R1	Louisenhoj	andesite	18°20'55"	64°46'25"	42.1 ± 0.6
SJ748R	Water Island	andesite	18°21'31"	64°42'05"	38.6 ± 0.8
SJ765R1	Water Island	rhyolite	18°19'23"	64°43'52"	30.9 ± 0.3

gastropods, echinoids, and corals (Donnelly, 1966) The presence of *Caprinuloidea* puts the origin in Albian time (113–97.5 Ma).

In the U.S. Virgin Islands, the Congo Cay Limestone Member (of Donnelly, 1959) of the Tutu Formation is a light gray recrystallized limestone found only on Congo Cay.

The Hans Lollik Formation crops out over the entire island of Hans Lollik. This formation consist of augite andesite, pyroclastic to epiclasic in origin. The Hans Lollik Formation is very similar in texture and composition to the Louisenhoj Formation.

Hydrothermal alteration is widespread along the southern shores of both St. Thomas and St. John and on many of the small islands along their coasts. Sericitic alteration is widespread throughout these two northern islands. Silicification is common and is especially well-developed on Red Point (St. Thomas) and Saba Island.

GEOLOGIC AGE

The rocks of St. Thomas and St. John have been mapped as a layered sequence. The Water Island Formation is the oldest; the rocks are younger to the north. The age given to the Water Island Formation is based on the age determined for the overlying Lower Cretaceous Coki Point Megabreccia lithofacies of Donnelly (1959) of the Tutu Formation that contains an Albian (97.5–113 Ma) fauna.

Two rocks from the Water Island Formation were dated by Donnelly (1966). One rock gave an age of 58–62±5 Ma but was presumed to have lost argon, and was discounted. A sample of hydrothermally altered rock gave an age of 106–110±10 Ma (Donnelly, 1966). This date agreed with the fossil evidence of Albian age in the overlying Coki Point Megabreccia lithofacies of the Tutu Formation and has been used as a minimum age for the Water Island Formation.

Five felsic rocks from the Water Island Formation on St. Thomas and St. John and two rocks of the Louisenhoj Formation from St. John were dated using the K-Ar whole rock technique (Tucker, 1987). The dating was done by Michael Diggles of the U.S. Geological Survey. The felsic rocks range in age from 65.8±2.9 to 30.9±0.3 Ma (table 2). Samples of the Louisenhoj Formation range in age from 42.1±0.6 to 37.7±1.1 Ma.

The rhyolite at site SJ685R lies between the mineralized zone on Bordeaux Mountain and a sulfide mineralized zone observed in drill cuttings from a nearby well. The absence of extensive alteration suggests that the rhyolite at site SJ685R was emplaced after the mineralization process, and thus represents a minimum age of mineralization in the immediate vicinity. Sample ST115R is only slightly altered along hairline fractures. Most of the rocks in the vicinity of sample site ST115R show signs of thermal alteration and mineralization. This sample of a small rhyolite plug may indicate a minimum age of mineralization (41 Ma) in the immediate vicinity.

Intrusive rocks on Puerto Rico range in age from 126 to some 37 Ma (Cox and others, 1977) with copper metallization being spatially related to quartz diorite and quartz diorite porphyry, which was determined to be about 40 Ma (Cox and others, 1977). This age is coincident with the minimum age of mineralization postulated for St. John, and possibly St. Thomas, and probably indicates a regional mineralization process.

In the British Virgin Islands, hornblende and biotite from the granodiorite on Virgin Gorda were dated at 34.2 and 36.3 Ma respectively (Cox and others, 1977). One sample of the Narrows pluton (of Donnelly, 1966) was dated at 24.3±0.3 Ma (Kesler and Sutter, 1979). These ages are consistent with the rocks dated during this study (table 2).

A continuous band of garnet-epidote skarn crops out on the Cays and extends to Mary Point on St. John.

Development of the garnet-epidote skarn is more pronounced in the southern exposures and decreases northward. This skarn metamorphism and marbleization (marmorization) continue on to Tortola (Helsley, 1960). The presence of a skarn mineral assemblage and marble in the sedimentary rocks reflects a thermal metamorphism. The Congo Cay Limestone Member of Donnelly (1959) of the Tutu Formation has the textural appearance of having been thermally recrystallized. On Tortola (British Virgin Islands), the contact between the skarn and marble and the Congo Cay Limestone Member is apparently gradual (Helsley, 1960). Geological observations and the geochemical data indicate that metamorphism occurred before periods of significant mineralization.

On Mingo Cay, a 1.5 m wide iron oxide dike cuts the marmorized rocks. This dike shows no indication of having been deformed or altered, indicating dike emplacement probably occurred after uplift of the sedimentary beds.

A small gabbroic body occurs in a basin south of Mary Point. A recent road cut near the top of the hill within the basin exposed a fault contact between the Tutu Formation and the gabbro. No evidence could be found that would indicate that the gabbro crystallized in place. Examination of the gabbro by SEM (scanning electron microscope) revealed the presence of minute veinlets of AgI and barite. This mineralogical assemblage is found throughout St. Thomas and St. John in association with hydrothermal mineralization. These observations indicate that the gabbro was in place before the mineralization occurred.

SAMPLE COLLECTION

Samples collected for this study include rock, soil and stream-sediments. Stream-sediment samples were collected primarily from third-order streams. Soil samples were collected within a 20 m radius of the stream-sediment sites and in intervening areas when additional sampling detail was required. Outcrop samples were collected at stream-sediment and soil sites, when available, and in areas of special interest. A total of 605 stream-sediments, 632 soils, and 817 outcrop samples were collected on all three islands.

Stream-sediment samples were collected as a composite of material over a 2–5 m length of the stream. Two samples were collected at each site: a 450 gm sample for sieving and a 4.5 kg sample for heavy mineral separation. Soil samples were generally collected at a 20–30 cm depth, generally within the B horizon. But, commonly, no distinct A-B horizon differentiation could be seen. In some instances bedrock was encountered before a distinct B horizon.

Rock samples were collected as composited 450 gm chip samples. Larger quantities of sample material were collected at visibly altered or mineralized outcrops.

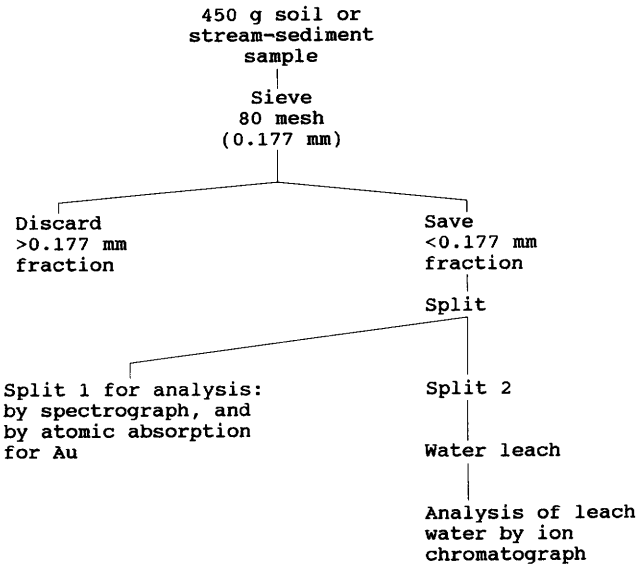

Figure 5. Sample preparation flow sheet for soil and stream-sediment samples.

SAMPLE PREPARATION

All sample types were heated for 6 hours at 120° C in the U.S.G.S. Denver laboratories in accordance with the U.S. Department of Agriculture regulations.

Figure 5 shows the sample preparation flow sheet for the 450 gm stream-sediment and soil samples; figure 6 shows a flow sheet for the 4.5 kg stream-sediment and soil samples; and figure 7 shows a flow sheet for the rock samples.

The oxalic acid leachates were prepared by bringing 5 gm of the bromoform light fraction to a boil in 20 ml of 5% oxalic acid and boiling for 10 minutes. The hot solution was filtered through a no. 41 Whatman filter, and the filtrate was brought to dryness on a hot plate. The resultant material was heated for 4.5 hrs. at 450° C in a muffle furnace to convert the oxalates to oxides. The oxides were then homogenized by mortar and pestle prior to analysis (Alminas and Mosier, 1975).

The water-leach extractions were performed by placing 1 gm of soil in a test tube with 10 ml of deionized water. The water and soil were thoroughly mixed and the test tube was placed on its side. The test tubes were remixed every second day. The samples were centrifuged after 8 days and the water decanted into a clean test tube for analysis.

ANALYTICAL TECHNIQUES

The U.S. Virgin Island samples, collected for the purpose of this study, were analyzed by a number of analytical techniques. Table 3 lists the analytical techniques used for

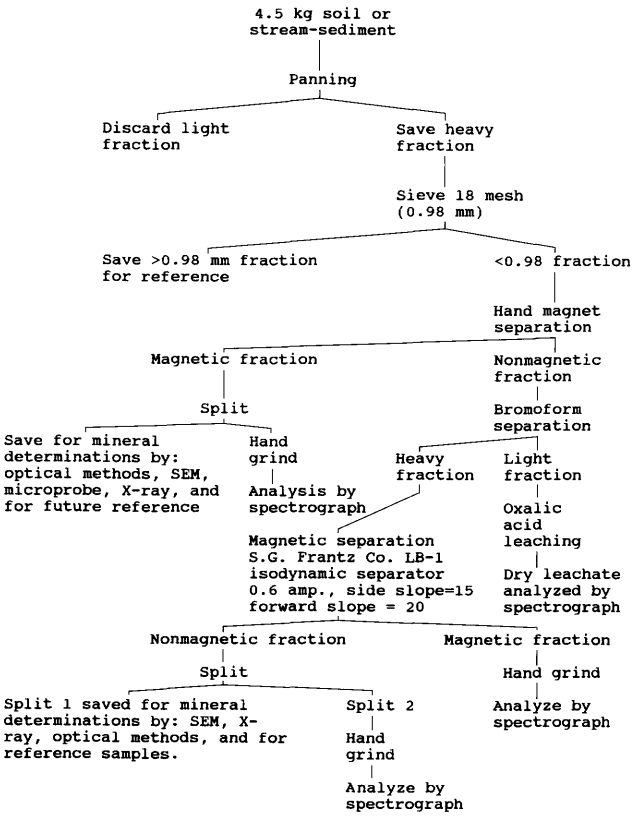

Figure 6. Sample preparation flow sheet for heavy mineral concentrates of soil and stream-sediment samples.

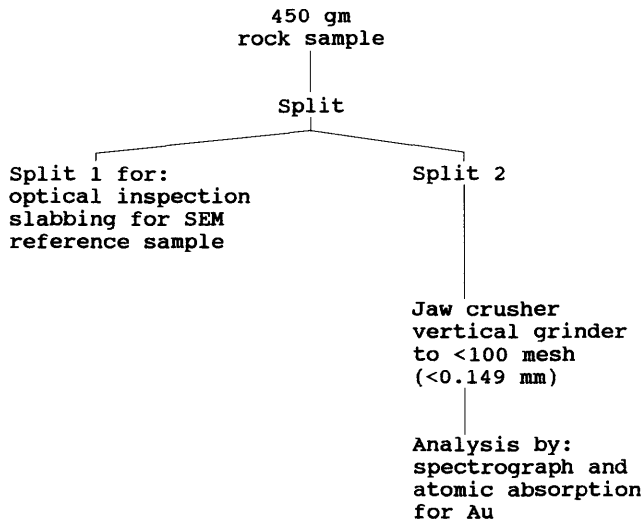

Figure 7. Sample preparation flow sheet for outcrop samples.

studying the different sample types. As can be seen, all the bulk sample types (rocks, <80 mesh soils, <80 mesh stream-sediments) were analyzed by the six-step D.C.-arc semiquantitative emission spectrographic method (Grimes and Marranzino, 1968) for thirty-one elements. In addition, they were analyzed for Au by flame (rocks) or flameless (soils and stream-sediments) atomic absorption methods. The three heavy mineral concentrate fractions and the oxalic acid leachates were analyzed by a modified six-step D.C.-arc semiquantitative emission spectrographic method. All of the resultant data has been published in two U.S. Geological Survey Open-File reports by Hopkins and others (1986) and McHugh and others (1989).

A Cambridge scanning electron microscope with energy dispersive spectrometry (Tracor Northern) capability was used to examine numerous rock slabs, bulk rocks, and processed samples. Electron microprobe analyses were done on an ARL SEMQ (scanning electon microscope quantitative) instrument using both natural and synthetic standards. Operating conditions were 15 or 20 Kv, 20 second count times on peaks, 4 second count times on background positions, spot size 1 to 5 microns. X-ray diffraction studies were done using Chas. Supper 114.6 mm Gandolfi cameras, and Pillips generator at 40 Kv, 30 Ma, CuKα radiation.

Major element analyses were performed using a Philips PW/600 simultaneous x-ray spectrometer that has a Rh end-window x-ray tube operating at 35 Kv and 60 Ma. Calibration was done using glass disks of 32 reference samples. A deJongh model was used for matrix corrections. The Abbey compilation (Abbey, 1980) of the best values for major oxides was used for all calibrations. A more detailed discussion of the procedure may be found in Taggart and others (1987).

GEOCHEMISTRY

GENERAL

This geochemical study of the U.S. Virgin Islands has delineated a previously unknown precious-metals and lead-tin metallogenic province in the northeastern portion of the Greater Antilles island arc. The mineralization detected on these islands (St. Thomas, St. John, and St. Croix) is characterized by an identical geochemical association consisting of Au, Ag, Te, Sn, Pb, Cu, Zn, Ni, Cr, Sb, As, Mo, Cl, and Ba. Although the geochemical association is common to all three islands, the inter-element ratios and overall anomaly intensities vary from island to island and from anomaly to anomaly.

The nonmagnetic fraction of the heavy mineral concentrates was the most effective sample medium in detecting the base-metal portion of the mineralization (fig. 8); whereas, low-level (ppb range) gold determinations of <80 mesh materials were effective in delineating the precious metals aspect. Water leaching of soils and the oxalic acid leaching of the bromoform lights fraction were useful in determining the mobility of elements in the secondary environment.

The REM (relative element magnitude) (VanTrump and Alminas, 1978) program was used in comparing the associations and mineralization intensities between the

Table 3. Analytical techniques used in the study of the U.S. Virgin Islands samples

Sample type	Analytical technique	Source or remarks
Outcrop source	Six-step D.C.-arc semiquantitative emission spectrographic method	Grimes and Marranzino, 1968; Meier, 1980.
	Flame atomic absorption method for Au	Meier, 1980.
< 80 mesh soils	Six-step D.C.-arc semiquantitative emission spectrographic method	Grimes and Marranzino, 1968.
	Flameless atomic absorption method for Au	Meier, 1980.
< 80 mesh source	Six-step D.C.-arc semiquantitative emission spectrographic method	Grimes and Marranzino, 1968.
	Flameless atomic absorption method for Au	Meier, 1980.
Nonmagnetic fraction	Modified six-step D.C.-arc semiquantitative emission spectrographic method	Grimes and Marranzino, 1968.
Magnetic fraction	----------Do----------	----------Do----------
Magnetite fraction	----------Do----------	----------Do----------
Oxalic acid leachates	----------Do----------	Alminas and Mosier, 1976; Grimes and Marranzino, 1968.
Major element analyses	X-ray fluorescence method	Taggart and others, 1987.

islands as well as between the major anomalies within an island. The REM program is designed to rank the magnitudes of individual element anomalies within a multielement geochemical anomaly. Calculations are performed on a cell basis rather than on individual sample sites. These calculations are performed on the basis of two parameters for each of the elements within the selected elemental suite. The first of these, the intensity factor, is derived by dividing the mean of all anomalous values of a given element within the defined area by its corresponding threshold value. The second, the area factor, is derived by dividing the number of sample locations within the defined area that contain anomalous levels of this element by the total number of sample locations within this area. The intensity and area factors are multiplied for each element and the product is the individual element magnitude (EM). All individual element magnitudes are added to give the total anomaly magnitude of the cell. In addition, each individual element magnitude is divided by the anomaly magnitude of the cell and the quotient is expressed in percent. This is the relative element magnitude (REM).

As per the data listed by Hopkins and others (1986) and McHugh and others (1989), the base-metal mineralization is most intense on St. Croix, especially with respect to Sn, Pb, Ni, Cr, and Sb. Silver, in the nonmagnetic fraction, is also most widespread on this island. The evidence for gold mineralization on St. Croix in rock and soil samples is the weakest of the three islands. St. John is intermediate in base-metal and gold mineralization and is characterized by the highest concentrations of copper and barium. St. Thomas shows the

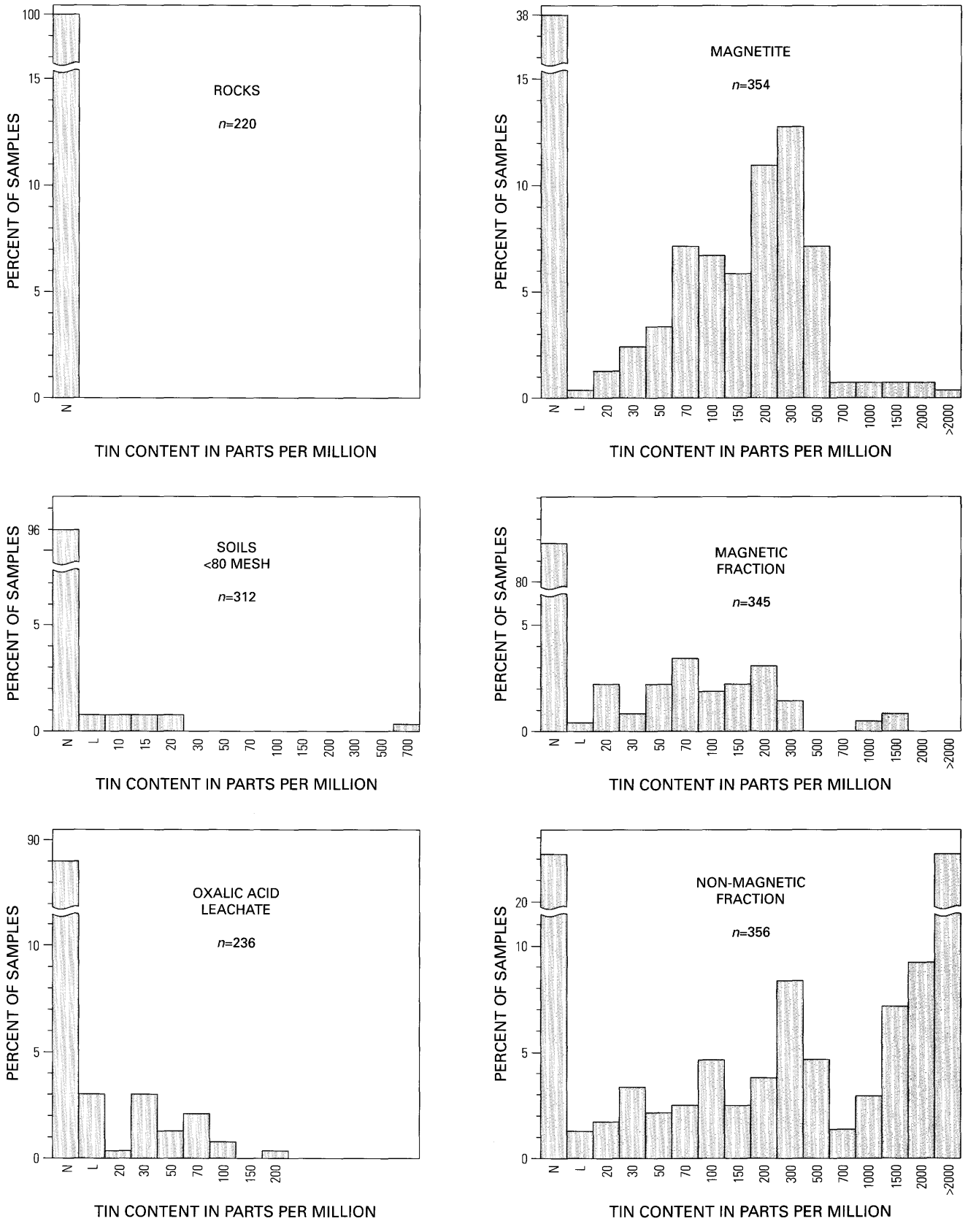

Figure 8. Histograms comparing tin concentrations in six sample media from St. Croix. L indicates that the metal was detected but at a concentration below the lowest indicated value. N indicates that the metal was not detected.

Table 4. Proportional distribution of tin, lead, gold, and silver in the U.S. Virgin Islands

Locality	Sn (NM-1)	Pb (NM-1)	Au (rock)	Au (soil)	Ag (rock)
St. Croix	54	42	9	25	1
St. John	34	26	27	33	45
St. Thomas	12	26	64	42	54

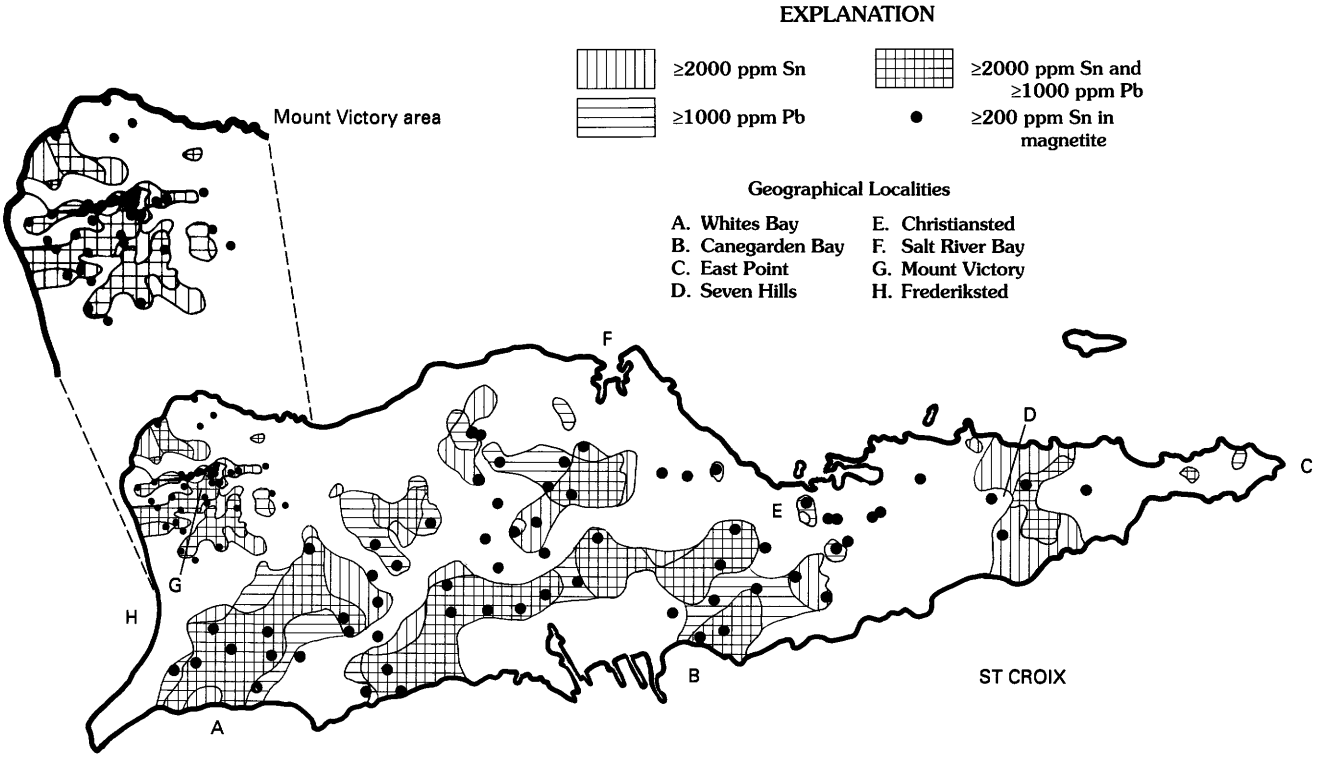

Figure 9. Tin and lead distribution in the nonmagnetic fractions of heavy mineral concentrates and in magnetites on St. Croix.

least evidence for base-metal mineralization, but evidence from rock and soil samples rank this island highest in gold mineralization (table 4).

The base-metal mineralogy in the secondary environment of these islands is unique. Tin occurs primarily in native form, as a tin or tin-lead chloride, or in the form of romarchite (SnO), and poorly crystallized cassiterite. Lead occurs in the native form, as cerussite, as tin-lead chloride(s), as lead chloride(s), and, rarely, as galena. Copper occurs in the native form, as a copper-tin alloy, as paratacamite ($Cu_2(OH)_3Cl$), as one of the oxides, and rarely as chalcopyrite. Nickel occurs primarily in the form of gersdorffite (NiAsS).

Gold occurs primarily in native form, as electrum, and as gold and gold-silver tellurides. Silver occurs primarily in the form of silver sulfide, silver iodide, silver chloride, and as silver and silver-gold tellurides. Commonly, the silver sulfide contains areas of disseminated ultrafine gold particles. The mineralogy will be discussed in detail later in this report.

ST. CROIX

The most extensive and intense tin and lead anomalies occur on the island of St. Croix (fig. 9). Here tin is detected in the nonmagnetic fraction at a 20 ppm level at 78 percent of the concentrate sample sites and at a concentration of ≥2000 ppm at 33 percent of the sites. Lead is found at concentration of ≥1000 ppm at 31 percent of the sites. Tin in magnetite occurs at a concentration of ≥200 ppm at 34 percent of these sites.

The most extensive base-metal anomalies on this island occur (west to east) in the Mt. Victory area, along the western graben wall (Whites Bay to Salt River Bay), along the

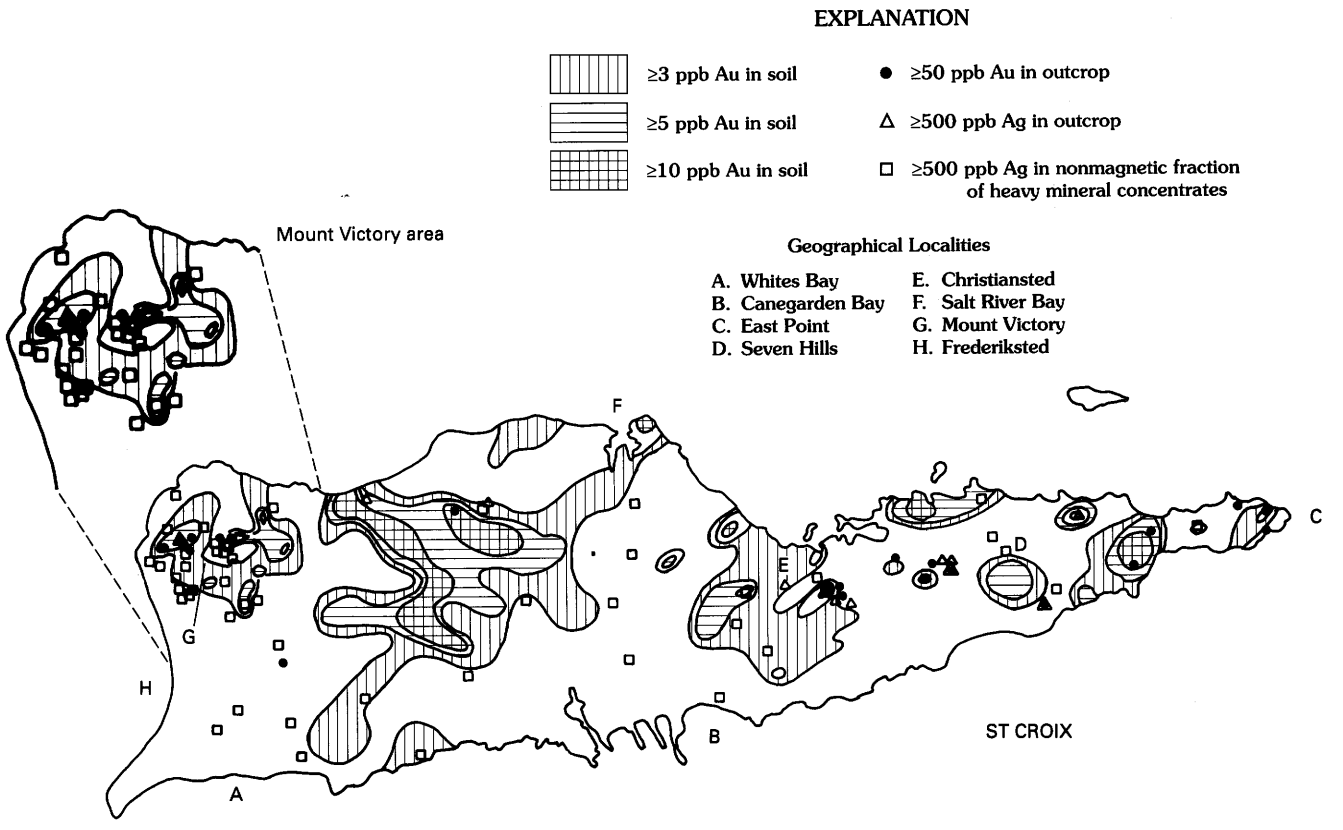

Figure 10. Gold distribution in B-horizon soils and rocks on St. Croix.

eastern graben wall (Canegarden Bay to Christiansted), in the Seven Hills area and at East Point (figs. 9 and 10).

Although the gold anomalies on St. Croix are less intense than those on St. Thomas and St. John, gold in soils occurs at the 3 ppb level at 43 percent of the sites and at the 10 ppb level at 8 percent of the sites. These gold anomalies delineate essentially the same areas on this island as do the base-metal anomalies.

The Mt. Victory anomalous area, in the northwestern corner of St. Croix (fig. 10), occurs in an area underlain by rocks of the Caledonia, the Allandale, the Cane Valley, and Judith Fancy Formations. The structural setting in this area is complex. The Annaly syncline occurs in the north and the Prosperity thrust in the south (fig. 2). As a whole, the area is characterized by extreme shearing. Small quartz and epidote veins are common and a number of small, unmapped intrusives occur throughout the area. Hydrothermal alteration is evident although strongly masked by pervasive weathering.

The base- and precious-metals anomalies in this area are nearly coextensive. The Mt. Victory anomaly has the highest overall values on the island with an EM value of 20,213. The prorated association relationship (REM) is shown in figure 11*A*.

The Mt. Victory area has a soil-gold EM value of 92, and thus ranks third within this island. On an inter-area basis, this area ranks first in lead (EM=7258) and copper (EM=1451) contents.

The Whites Bay–Salt River Bay anomaly, which inludes both base- and precious-metals, occurs in the west-central portion of the island and extends in a northeasterly direction from Whites Bay, in the southwest, to Salt River Bay in the northeast (fig. 9). This anomaly extends along the western wall of the St. Croix graben and is underlain by rocks of the Judith Fancy Formation, the Jealousy Formation, and the graben-filling Kingshill Limestone. This area is also structurally complex. In addition to the northeast-trending graben wall one major anticline and two synclines occur at right angles to the graben in the northern portion of the anomaly. The Coble syncline and a parallel unmapped structure, farther to the north, are characterized by intense gold anomalies in the soils (figs. 2 and 10).

A zonational aspect between the base- and precious-metals anomalies is evident at the Whites Bay–Salt River Bay anomaly. The gold-rich areas occur centrally (figs. 2 and 10) and the base metal anomalies form a halo around them (figs. 9 and 10). This is the second most intense base-metal anomaly on the island with an EM value of 13,518. The prorated association relationship for this area is shown in figure 11*B*.

The soil-gold anomaly value for this area ranks first within this island with an EM value of 423. On an inter-area

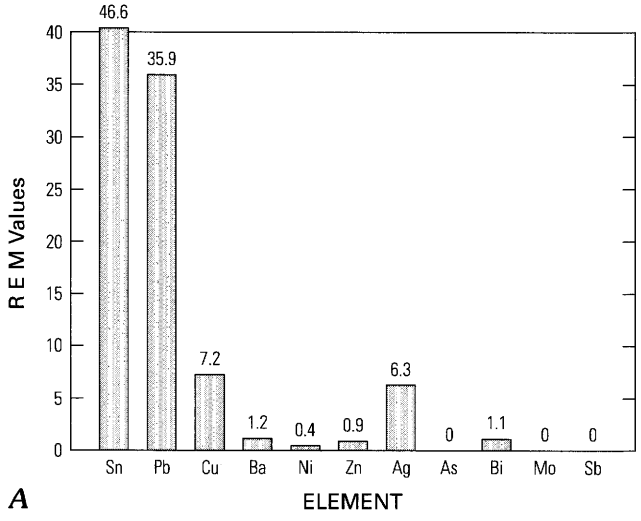

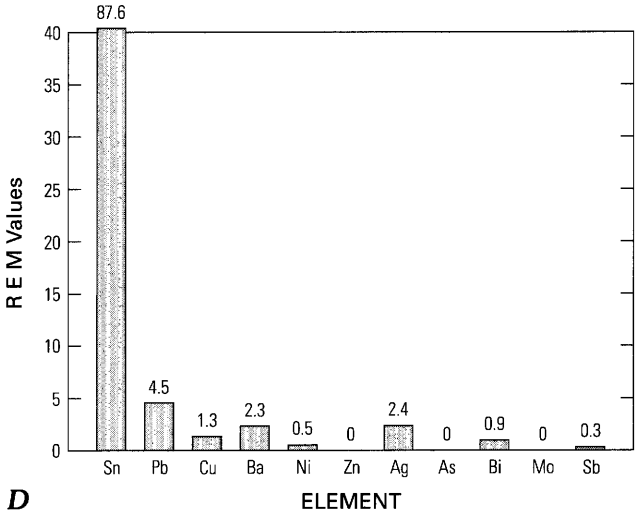

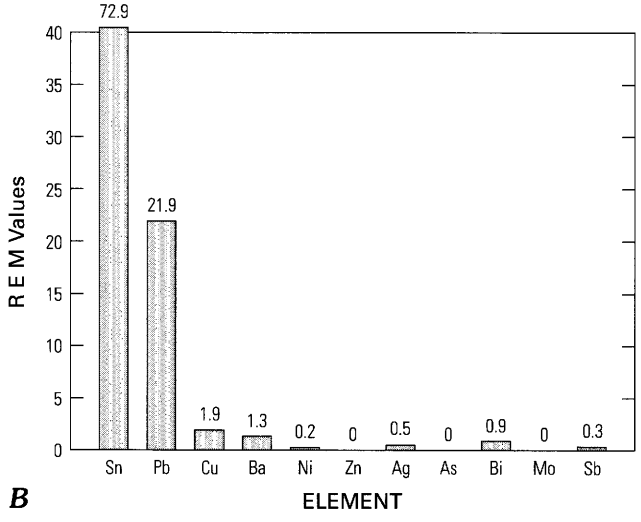

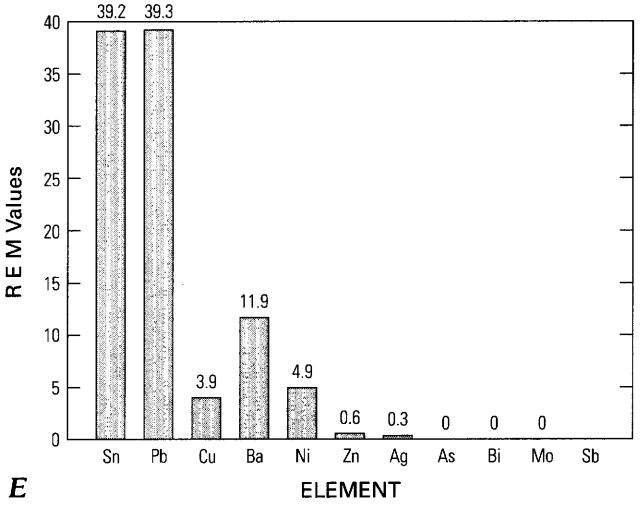

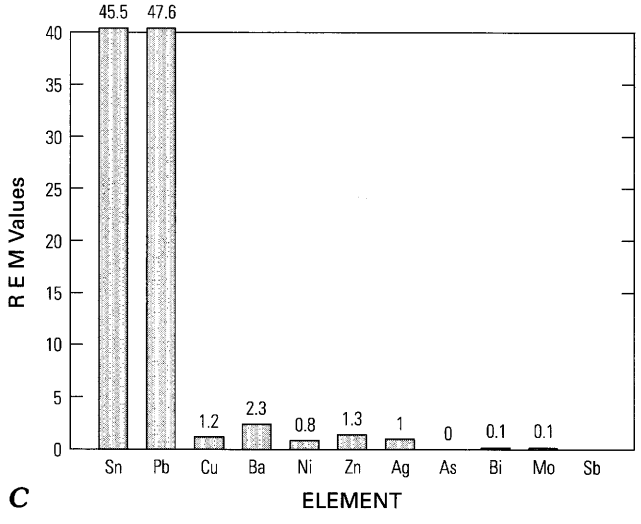

Figure 11. Association relationships for five geochemical anomalies on St. Croix. *A*, Mt. Victory area; *B*, Whites Bay–Salt River Bay; *C*, Canegarden Bay–Christiansted; *D*, Seven Hills area; *E*, East End.

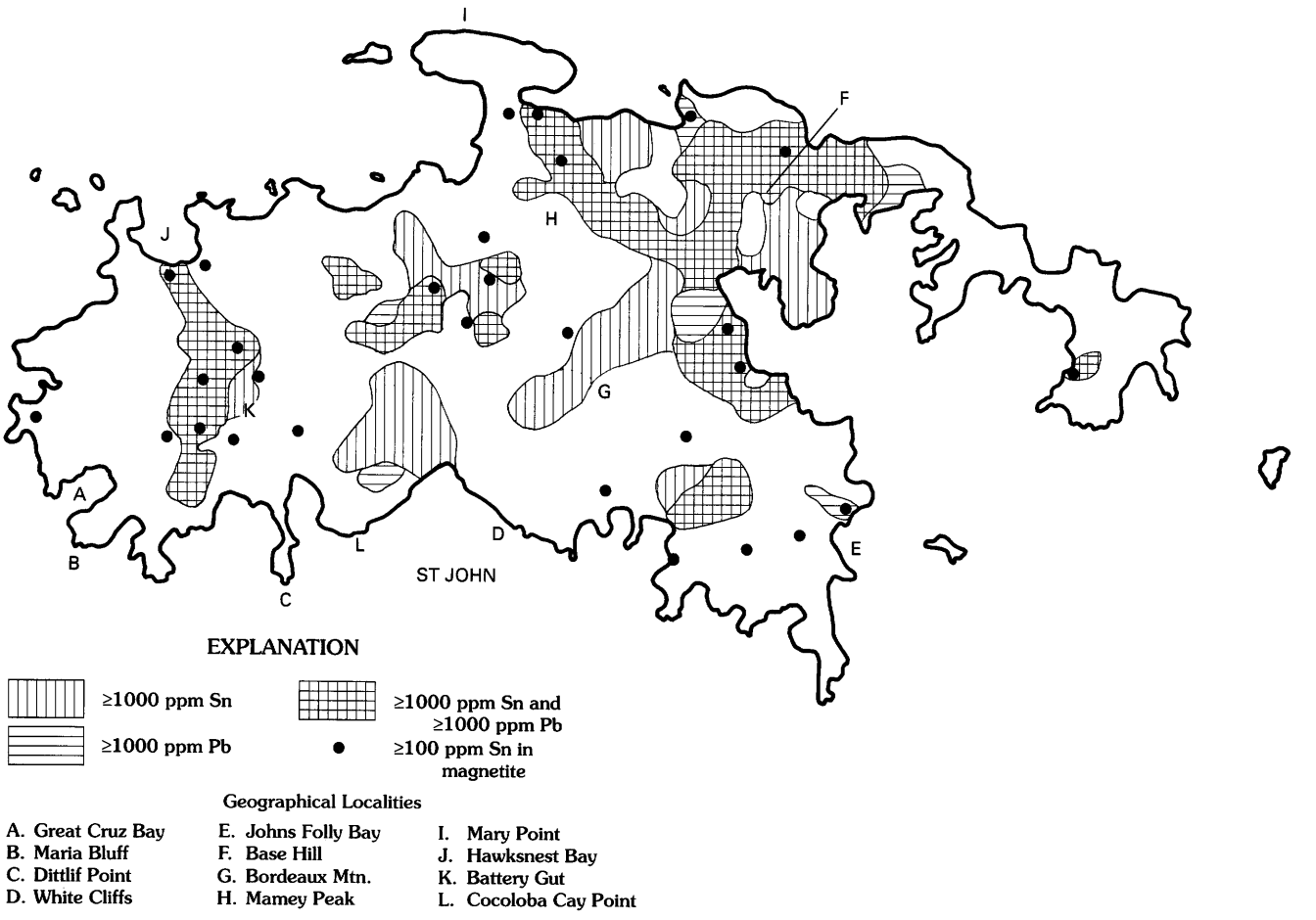

Figure 12. Tin and lead distribution in the nonmagnetic fraction of the heavy mineral concentrates and in magnetites on St. John.

basis, this anomaly also ranks first in tin (EM=9849) content.

The Canegarden Bay–Christiansted anomalous area occurs in the central portion of the island (figs. 9 and 10) and extends from Canegarden Bay in the south to Christiansted in the north. This anomaly occurs over the eastern graben wall and is underlain by rocks of the Judith Fancy Formation to the east and the Kingshill Limestone to the west. The Kingshill Limestone is somewhat silicified and epidotized in the northeastern portion of the anomaly and tends to form hills. The gold anomaly is more intense in the northern portion of the area and the base-metals occur more in the south. This is the third most intense base-metal anomaly on the island with an EM value of 12,446. The prorated association relationship for this area is shown in figure 11*C*. This soil-gold EM value here is 76 and thus this area ranks third on St. Croix with respect to gold content.

The Seven Hills anomalous area is located in the eastern end of the island and is centered on the Seven Hills Range. The base-metal portion of the anomaly is continuous and occurs in the central portion of the area. The gold anomaly is quite fragmented and tends to form a halo in the outer portions and is underlain exclusively by rocks of the Caledonia Formation. This area is characterized by two northwest-trending anticlines and synclines (fig. 2). The base-metal anomaly ranks fourth in magnitude on St. Croix with an EM value of 6253. The prorated association relationship for this area is shown in figure 11*D*. The soil-gold anomaly intensity is at some variance with that of the base metals and ranks second for the island with an EM value of 189.

The East Point anomaly occurs at the extreme eastern tip of St. Croix. This area is characterized by a centrally located soil-gold anomaly with an intermittent, outer base-metal halo. The area is underlain by rocks of the Caledonia Formation exclusively and no major structures have been mapped here. This is the least pronounced of the five base-metal anomalies on St. Croix, with an EM value of 4838. The prorated association relationship for this area is shown in figure 11*E*. The soil-gold anomaly, here, is also the lowest on the island with an EM value of 52.

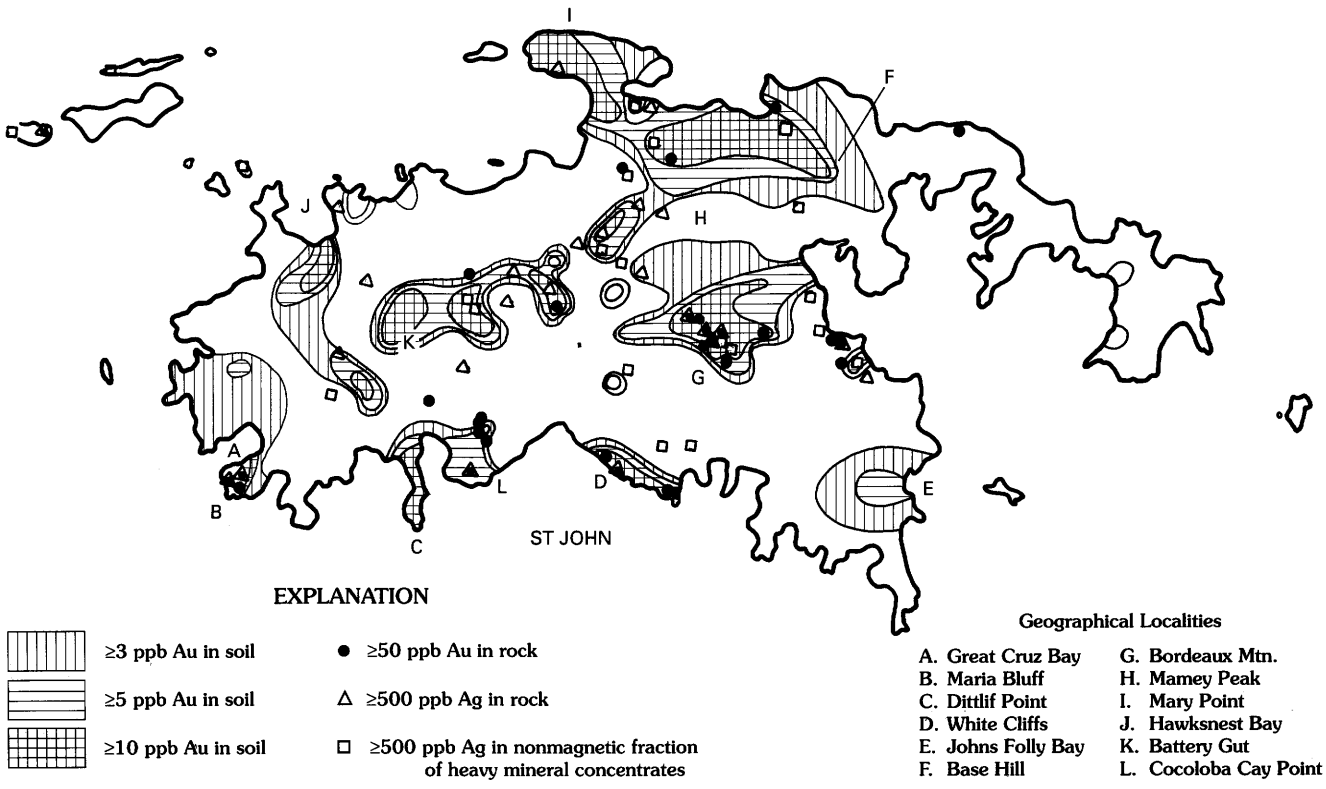

Figure 13. Gold distribution in B-horizon soils and rocks on St. John.

ST. JOHN

St. John ranks second in the intensity and extent of base-metal anomalies among the three islands. Here, tin is detected in the nonmagnetic fraction at a 20 ppm level at 52 percent of the concentrate sample sites and at a concentration of ≥2000 ppm at 19 percent of the sites (fig. 12). Tin in magnetite occurs at a concentration of ≥200 ppm at 12 percent of these sites.

The most extensive base-metal anomalies on this island occur (west to east) in the Hawksnest Bay–Dittlif Point area, the Battery Gut–Mamey Peak area, The Mary Point–Base Hill area, and the Bordeaux Mountain area (fig. 12).

The soil-gold anomalies on St. John are more intense than those on St. Croix. Gold in soils occurs at the ≥3 ppb level at 45.6 percent of the sites and at the ≥10 ppb level at 18.5 percent of the sites. These gold anomalies occur in generally the same areas as the base-metal anomalies (compare figures 12 and 13).

The Hawksnest Bay–Dittlif Point anomalous area occurs near the western end of the island (fig. 12), and is underlain predominantly by rocks of the Louisenhoj Formation. A major northeast-trending fault cuts the central portion of this area. Pronounced hydrothermal alteration is visible on Dittlif Point and the first peninsula to the east. In addition, this peninsula is characterized by the presence of abundant sulfides in the outcrops.

The base-metal and soil-gold anomalies in this area are nearly coextensive. Of the four calculated areas on St. John, this area has the lowest base-metal EM value at 8411. The prorated association relationship is shown in figure 14*A*. The EM value for the soil-gold anomaly for this area is 342, which is the second lowest for this island, although it would rank just below that of the western graben wall anomaly on St. Croix.

The Battery Gut–Mamey Peak anomaly extends along a major northeast trending fault in the central portion of the island. This area is underlain in equal parts by rocks of the Louisenhoj Formation to the north and the Water Island Formation to the south of the fault. The extensive zone of hydrothermal alteration occurring along this zone is frequently masked by pervasive weathering. The base-metal anomaly here is somewhat more areally restricted than the soil-gold anomaly, but it still has an EM value of 13,913. The prorated association relationship for this area is shown in figure 14*B*. The soil-gold anomaly in this area has the lowest EM value for this island with a value of 228. This EM value would rank this area second highest as compared to the anomalies on St. Croix.

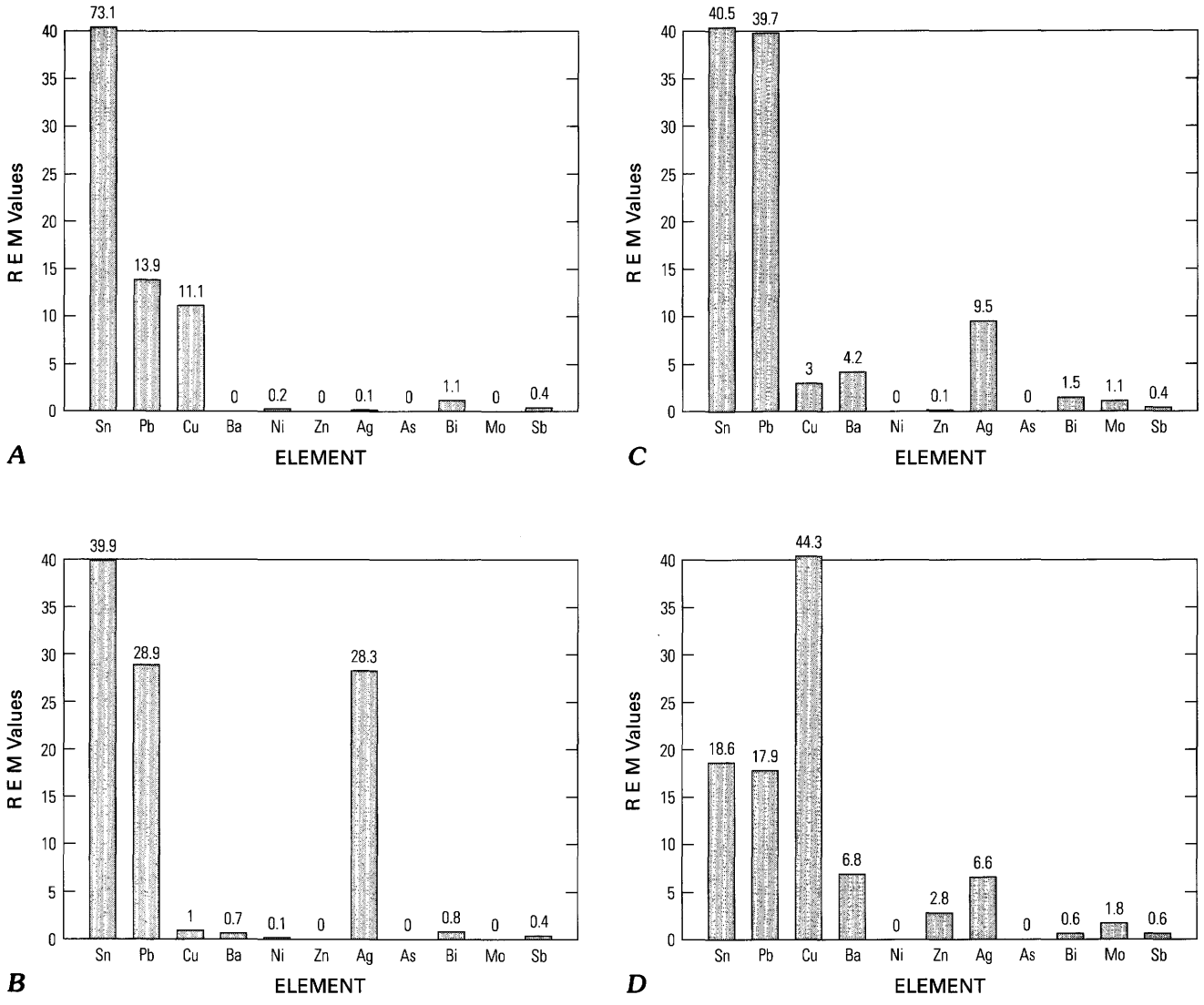

Figure 14. Association relationships for four geochemical anomalies on St. John. *A*, Hawksnest-Ditliff Point; *B*, Battery Gut–Mamey Peak; *C*, Mary Point–Base Hill; *D*, Bordeaux Mountain.

The Mary Point–Base Hill base-metal anomaly incorporates the largest area on St. John, which is also true for the soil-gold anomaly occurring here. This area is complex both geologically and structurally; the area is underlain by rocks of the Louisenhoj Formation, the Outer Brass Limestone, rocks of the Tutu Formation and dioritic rocks. The area is cut by major northwest- and northeast-trending faults—some of which show a spatial relationship to the geochemical patterns. Pronounced hydrothermal alteration is visible here, though it is frequently obscured by the pervasive weathering. The area incorporates the most intense base-metal anomaly on St. John with an EM value of 17,388. The prorated association relationship is shown in figure 14*C*. The soil-gold anomaly here has an EM value of 397 and is thus the second most intense on the island. On an inter-area basis, this area has by far the highest EM values for tin, lead, and silver.

The Bordeaux Mountain area is located in the east-central portion of the island. Here, the base-metal and soil-gold anomalies center on the gossan-capped Bordeaux Mountain. This area is underlain exclusively by rocks of the Water Island Formation with little or no structural features noted in this area. The Bordeaux Mountain gossan is at least 7 m thick and reveals no replacement texture. The base-metal and soil-gold anomalies are essentially coextensive. This is the second most intense base-metal anomaly on St. John with an EM value of 16,884. The prorated association relationship here is

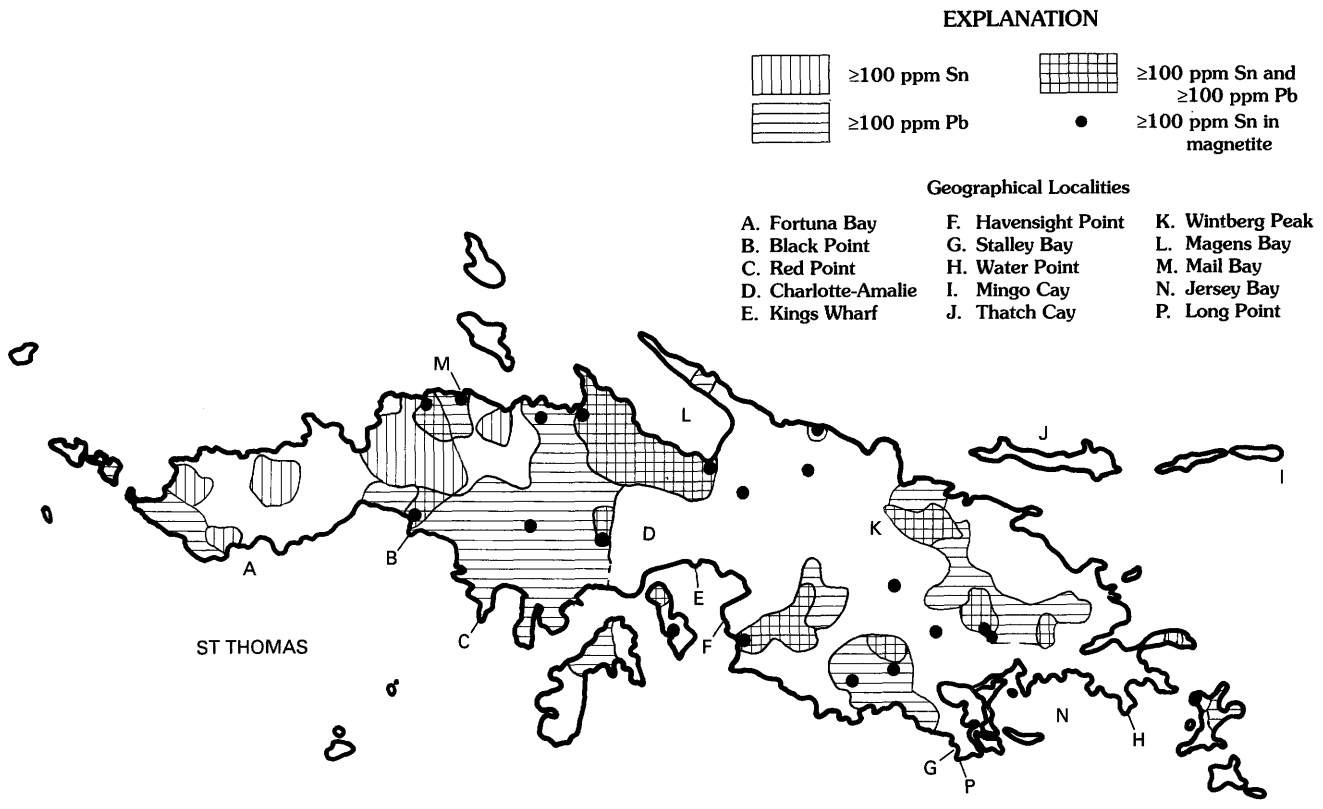

Figure 15. Tin and lead distribution in the nonmagnetic fraction of heavy mineral concentrates and magnetites on St. Thomas.

shown in figure 14*D*. The soil-gold anomaly here ranks first in intensity on St. John with an EM value of 468.

In addition to the above delineated areas, three smaller anomalies occur along the southern St. John coast. The westernmost of these occurs at Maria Bluff–Great Cruz Bay. This area is characterized by gold and silver anomalies. Here, a sample of a strongly altered siliceous intrusive contained 5.5 ppm gold and abundant lead-rich jarosite.

The White Cliffs area, to the east of Dittlif Point, consists primarily of a fine-grained hydrothermal quartz with minor amounts of alunite and is capped by a thin siliceous gossan. The quartz contains low levels of gold and silver as well as copper in the form of chalcopyrite. Turquoise veins occur along minor fractures and the cliffs are coated with native sulfur and paratacamite.

The last minor anomaly occurs at Johns Folly Bay, along the east coast of St. John. This area is characterized by strong hydrothermal alteration.

An east-west trending string of small islands occurs to the north of and between St. John and St. Thomas. These islands are named (west to east) Thatch Cay, Grass Cay, Mingo Cay, Lovango Cay, Congo Cay, and Whistling Cay (figs. 3 and 4). This string of islands represents a skarn zone extending into Mary Point on St. John. Fine-grained marble and garnetiferous rocks are common between Mingo Cay (on St. Thomas) and Mary Point. This area is characterized by magnetite veins, copper-bearing barite and calcite veins, and low levels of gold and silver.

ST. THOMAS

Lead and tin anomalies are least pronounced on the island of St. Thomas (fig. 15). Here tin is detected in the nonmagnetic fraction at a 20 ppm level at only 55 percent of the concentrate sample sites and at a concentration of 2000 ppm at 13 percent of these sites. Lead is found at a concentration of 1000 ppm at 19.6 percent of the sites. Tin in magnetites occurs at a concentration of 200 ppm at 11 percent of these sites.

The most extensive base-metal anomalies on this island occur (west to east) in the Mail Bay–Black Point area (fig. 15), the Magens Bay–Kings Wharf area, the Havensight Point–Stalley Bay area and the Wintberg Peak–Water Point area (fig. 15).

In contrast with tin and lead, the soil-gold anomalies on St. Thomas are more intense than those on St. John or St. Croix. Gold in soils occurs at the 3 ppb level at 55 percent of the sample sites and at the 10 ppb level at 13 percent of the sites. These gold anomalies delineate essentially the same

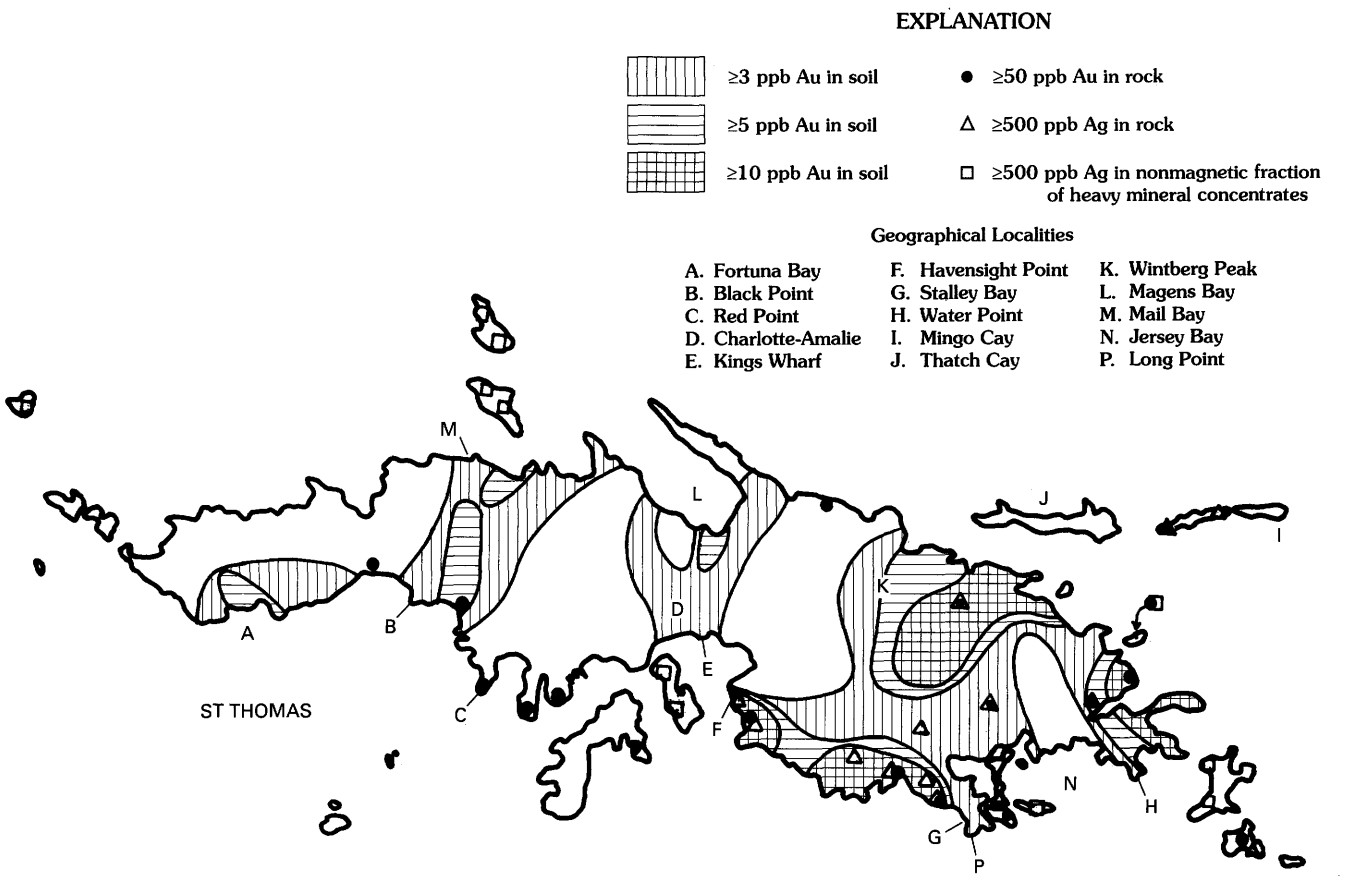

Figure 16. Gold distribution in B-horizon soils and rocks on St. Thomas.

areas on this island as do the base-metal anomalies, but they tend to be more extensive (fig. 16).

The Mail Bay–Black Point anomaly occurs to the west of Charlotte-Amalie. This area is underlain exclusively by rocks of the Louisenhoj Formation and no major structure was indicated here. The Harry S. Truman airport area, immediately to the southeast of this anomaly, was strongly altered and metallized. This airport area is characterized by malachite pods containing disseminated iodargyrite (silver iodide) and a small, iron-rich and extremely siliceous breccia pipe at Red Point. This material was being rapidly removed to be used as fill in the extension of the airport runway. The base-metal anomaly in this area is more extensive than the soil-gold anomaly. This area has the highest overall base-metal anomaly intensity on St. Thomas with an EM value of 12,928. The prorated association relationship here is shown in figure 17*A*.

The soil-gold anomaly for this area has an EM value of 73, which is the lowest for the island. On an inter-area basis, this anomaly ranks the highest in lead (EM=8395).

The Magens Bay–Kings Wharf anomaly is located in the vicinity of and to the north of Charlotte-Amalie. This area is underlain predominantly by rocks of the Louisenhoj Formation and, to a lesser extent, by the Outer Brass Limestone and rocks of the Tutu Formation in the north. No major structures are indicated in this area. Hydrothermal alteration is visible along the north shore. Generally, however, outcrop exposures over most of this area are poor.

This is the second most intense base-metal anomaly on St. Thomas with an EM value of 9858. The prorated association relationship for this area is shown in figure 17*B*. The soil-gold anomaly ranks second on St. Thomas with an EM value of 96.

The Havensight Point–Stalley Bay area is located in the eastern part of St. Thomas along the southern shore line (figs. 15, 16). This is a geologically and structurally complex area. The area is underlain predominantly by rocks of the Water Island Formation intruded by a number of quartz-andesine porphyry dikes. Numerous major north- and northwest-trending faults cut the area. This area is characterized by the presence of quartz porphyry intrusives, pronounced and widespread hydrothermal alteration, and the presence of numerous epidote, quartz, and iron oxide veins. Some of these quartz veins are precious-metal rich, and one of these is 0.6 m (2 ft) thick with values as high as 20 ppm Au and several hundred parts per million silver. One epidote vein contains

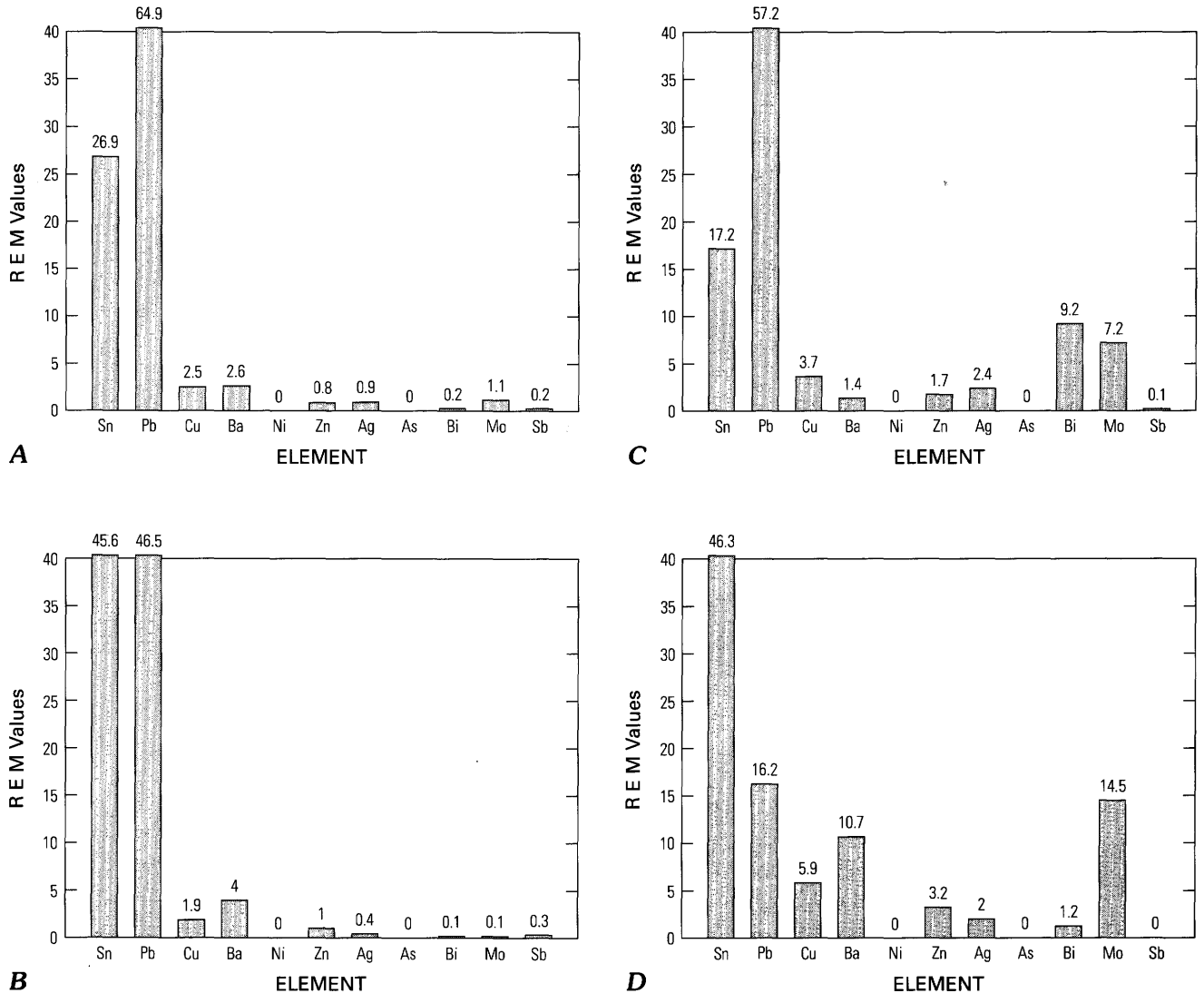

Figure 17. Association relationships for four geochemical anomalies on St. Thomas. *A*, Mail Bay–Black Point; *B*, Magens Bay–Kings Wharf; *C*, Havensight Point–Stalley Bay; *D*, Wintberg Peak–Water Point.

>200 ppm tellurium. Gossany material is abundant immediately to the southeast on Long Point. Very coarse iron oxide boxwork occurs in Jersey Bay, to the east of Stalley Bay. The base-metal anomaly in this area ranks fourth in intensity on St. Thomas with an EM value of 5909. The prorated association relationship is shown in figure 17*C*. The soil-gold anomaly is substantially more extensive and continuous than the base-metal anomaly. This area ranks second on St. Thomas in soil-gold content with an EM value of 1247.

The Wintberg Peak–Water Point area is located along the northeastern St. Thomas shore. This area is underlain by a wide range of rock types. In the southern part of the area, rocks of the Water Island Formation are cut by numerous northeast-trending dikes of quartz-andesine porphyry. South to north, the area is underlain by rocks of the Louisenhoj Formation, the Outer Brass Limestone, and the Tutu Formation. The area is bounded to the west by a major northwest-trending fault. Pronounced hydrothermal alteration is visible along the coastal portion of this area. Iron introduction is very visible—as the name Redhook Point (north of Water Point; fig. 4) implies. The base-metal anomaly is substantially less extensive and is located centrally within the soil-gold anomaly here (figs. 15, 16). This is the least intense base-metal anomaly on St. Thomas with an EM value of only 3099. The prorated association relationship for this area is shown in figure 17*D*. The soil-gold anomaly here is more intense than any other area on all three islands with an EM value of 1414.

MINERALOGY

Until this study of the U.S. Virgin Islands, the presence of mineralization, the extent of this mineralization, and the mineralogy associated with it were totally unknown. Preliminary results were given by Foord and others (1988). Because of the complex elemental associations, the existing mineral assemblages are diverse. In addition, because of the depositional (hydrothermal and weathering) complexity, much additional work is necessary, particularly on the hydroxides, oxychlorides, oxide-hydroxides, and related compounds of lead and tin. However, a hitherto unrecognized mineral assemblage has been documented by this work. Table 5 lists the minerals and compounds identified in this study. Several aspects of the total mineralogy are particularly noteworthy.

NATIVE ELEMENTS AND ALLOYS

With regard to occurrence of the native elements, all are straightforward in terms of occurrence except for native tin and native lead. Relatively few worldwide occurrences of these two metals have been reported singly or combined (as alloys or intergrowths of the two metals) ([Sn] Lawrence, 1951; Silman, 1954; Aleksandrov, 1955; Turovsky, 1956; Hosking, 1974; Uwadiale and Hall, 1984; [Pb] Novgorodova and others, 1981; Krylova, 1975; Kucha, 1981; [Sn and Pb] Filimonova and others, 1981). Recently, what appear to be eutectic intergrowths and solid-solutions of lead and tin have been reported by Tomson and others (1989) and Okrugin and others (1981). Of all of the native metals found by us, tin and lead are the most common. Both of these metals, and others (such as native iron and aluminum), have been reported mainly from secondary and weathering environments as well as organic-rich environments and much less frequently from primary and/or hydrothermal sources. Some of the references given above document high temperature and pressure primary origins for native elements, for example, in rhyolite, andesite, syenite, and granite. We are well aware of the possibility that some of the native tin and lead found in the Virgin Islands may be man-made (from pewter); but for man-made materials, the mode of geologic occurrence, the trace element geochemistry, and the textures of samples differ markedly from what we conclude to be naturally occurring material. The existence of these metals here, as in other worldwide locations, strongly favor a natural origin for the two metals in all or nearly all of the occurrences.

Native tin and native lead frequently occur together as eutectoid intergrowths that are mantled by native tin that in turn is coated by a complex fine-grained mixture of lead and/or tin oxides, hydroxides, carbonates, oxychlorides, and other unidentified compounds (figs. 18, 19). Figure 20 shows a closeup view of the tin-lead eutectic intergrowth.

Table 5. List of minerals and compounds found to occur in the weathering environment in the U.S. Virgin Islands.

Native elements	Alloys	Tellurides
Gold	Electrum	Au-Te
Silver	Cu_6Sn_5	Au-Ag-Te
Copper	$Cu_{5.6}Sn$(?)	Ag-Te(?)
Tin		Bi-Te(?)
Lead		
Tellurium		
Bismuth(?)		
Sulphur		

Oxides and hydroxides	Sulfides
Chromite	Chalcocite
Cassiterite	Sphalerite
Romarchite	Acantite
Cuprite	Galena
Tenorite	Pyrite
Litharge	Marcasite
Minium	Chalcopyrite
Magnetite	Arsenopyrite
Maghemite	Gersdorffite
Hematite	
Ilmenite	
Rutile	
Goethite	
Lepidocrocite	

Halides and halogenides
Sn-Cl-OH/Sn-Cl-OH-H_2O/Sn-Cl-H_2O
Sn-Pb-Cl-OH/Sn-Pb-Cl-OH-H_2O/Sn-Pb-Cl-H_2O
Pb-Cl-OH/Pb-Cl-OH-H_2O/Pb-Cl-H_2O
Cotunnite
Paratacamite
Phosgenite
Chlorargyrite
Bromargyrite
Iodargyrite
Sylvite
Fe-Cl/Fe-Cl-OH/Fe-Cl-OH-H_2O bismoclite-daubreeite

Sulfates, phosphates, carbonates, and vanadates	Silicates (excludes common rock-forming minerals)
Barite	Epidote
Cerussite	Ni-silicate
Hydrocerussite	Y-silicate
Jarosite-plumbojarosite	Wollastonite
Apatite	Garnet group (chiefly andradite-grossular)
Turquoise	Phrenite
Monazite	
Pyromorphite	
Mottramite(?)	
Bismutite	
Alumite	
Malachite	

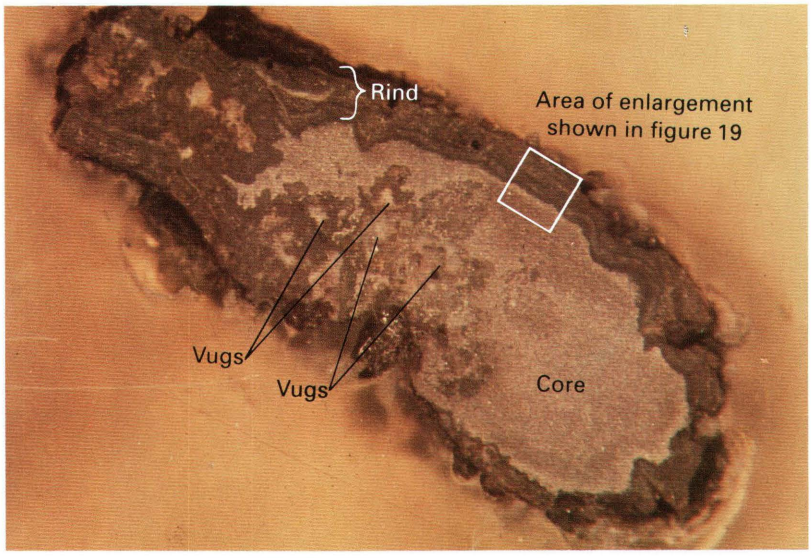

Figure 18. Photomicrograph of native tin-lead nugget (SC514) coated by a rind consisting of a complex, fine-grained mixture of lead plus tin oxides, hydroxides, and oxychlorides with fine blebs of native lead and tin. The core portion consists of a eutectoid intergrowth of native tin and lead. The vugs are filled with tin, tin-lead, or lead oxychlorides. Field of view = 9×4mm.

Table 6. Microprobe analyses of native tin and native lead nuggets occuring in eutectic or eutectoid intergrowths from the U.S. Virgin Islands, in weight percent

Nugget type	Native Sn	Native Pb			
Sample no.	SC514A	SJ601A	SC514	SJ601	29
Number of analyses.....	3	1	1	2	2
Sn	99.6	0.0	6.0	0.2	0.0
Pb	0.3	100.6	94.6	99.7	101.0
Total	99.9	100.6	100.6	99.9	101.0

Nuggets and masses of native lead with or without coatings of secondary oxides, carbonates, hydroxides, oxychlorides, and other unidentified compounds are uncommon, and comparable masses of native tin are rare. The majority of "native-metal appearing" nuggets and grains are actually mixtures of both metals plus a complex assemblage of lead-tin oxides, oxychlorides, carbonates, hydroxides, and other unidentified compounds. Only rarely are native tin and native lead found individually. Nuggets of all three types (Pb-Sn, Pb, Sn) are as much as 5 mm in maximum dimension. In many cases, the eutectic-like intergrowths are composed of native lead or tin (but not both) and cerussite, cotunnite, and other as yet unidentified oxychlorides and hydroxides (see figs. 21–25). The eutectic texture is also present within mixtures of lead-tin oxides, hydroxides, carbonates, oxychlorides, and other compounds (fig. 26). Euhedral crystals of Cu_6Sn_5 frequently occur within this complex mixture (figs. 27 and 28). Nuggets and masses may be panned or concentrated by heavy liquids from stream and colluvial sediments. Figures 18 and 19 show one of these zoned nuggets (SC514), and figures 29 and 30 are element distribution maps for tin and lead for an area within the eutectic portion of the same sample. Microprobe analyses for native tin and lead are given in table 6.

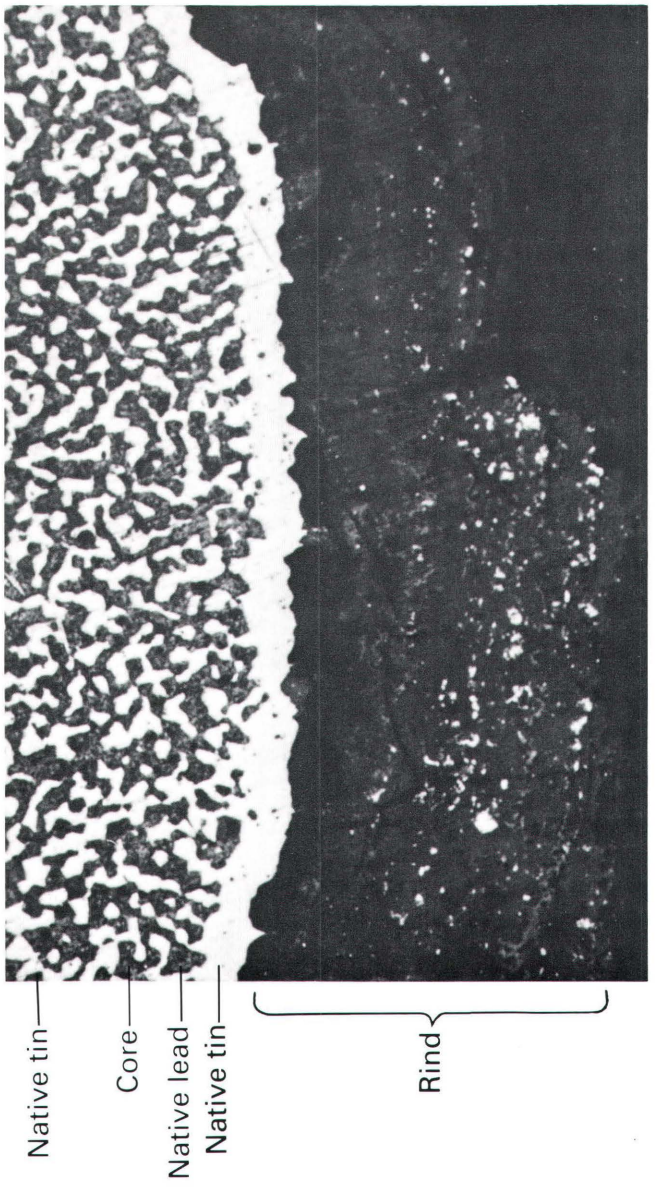

Figure 19. Photomicrograph showing detail of the eutectoid core portion and rind of the grain shown in figure 18, sample (SC514). Field of view = 2 × 1 μm.

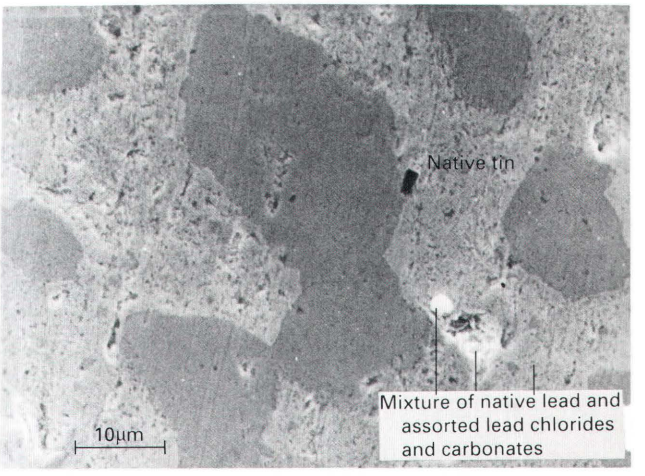

Figure 20. Scanning electron microscope (SEM) photomicrograph showing a closeup view of the eutectoid intergrowth of native tin and lead in the core portion of the SC514 nugget (seen in fig. 19). Scale bar = 10 μm.

Figure 21. Backscatter electron (BSE) photomicrograph of a portion of a lead-tin nugget (sample Box 10C) from the graben area on St Croix. This picture is of the same area shown in the map in figure 22. Scale bar = 5 μm.

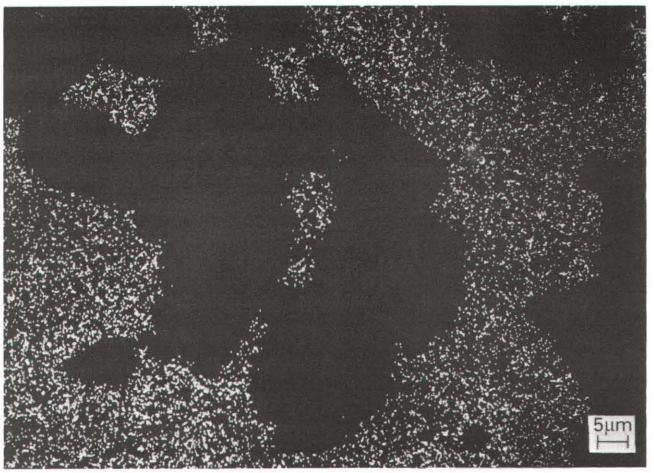

Figure 23. Element distribution photomicrograph (EDPM) map of lead in grain (sample Box 10C) shown in figure 21. Scale bar = 5 μm.

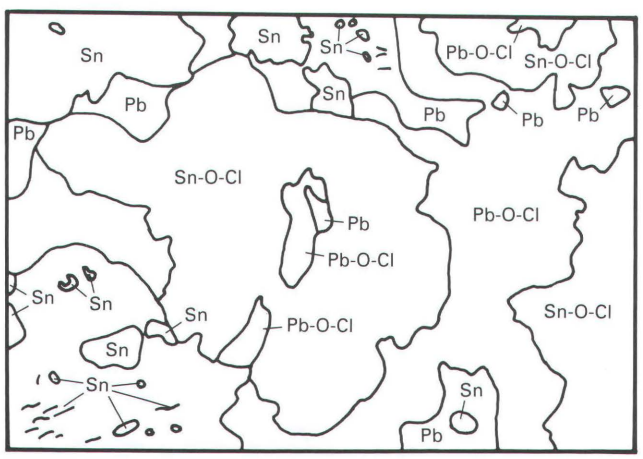

Figure 22. Compositional map of grain seen in figure 21 showing the mineralogic complexity common to the lead-tin nuggets. The various portions of the grain are identified by elemental content and not by chemical formula. Scale bar = 5 μm.

Figure 24. EDPM of chlorine in grain (sample Box 10C) shown in figure 21. Scale bar = 5 μm.

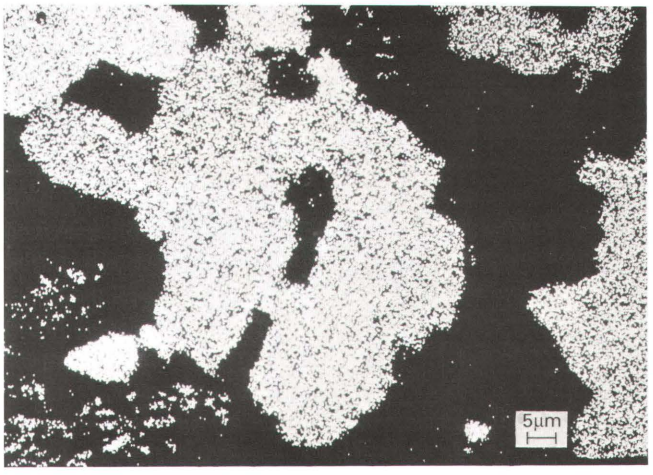

Figure 25 (facing column). EDPM map of tin in grain (sample Box 10C) shown in figure 21. Scale bar = 5 μm.

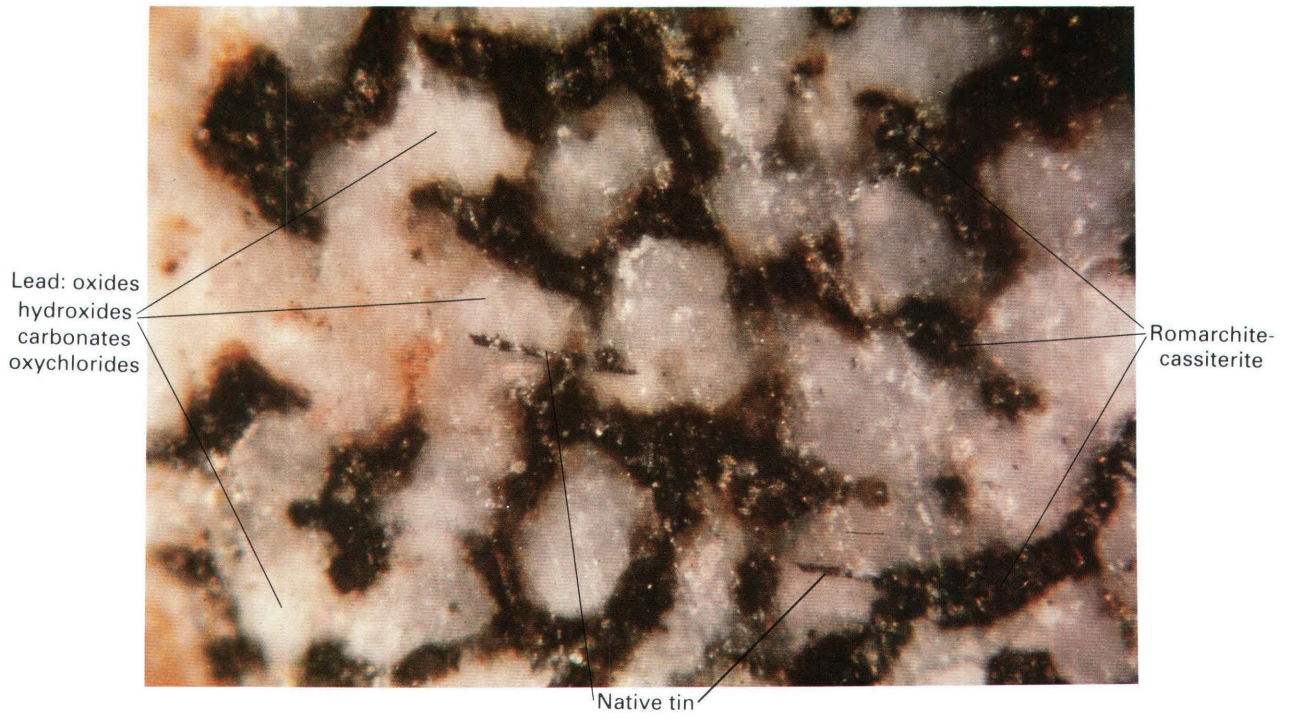

Figure 26. Photomicrograph of a mineral grain from St. John showing a eutectoid intergrowth of romarchite-cassiterite (dark brown portions) and lead oxides, hydroxides, carbonates, and oxychlorides (white portion). Metallic blade-like native tin can be seen cross-cutting the eutectoid texture. Field of view = 2×1 mm.

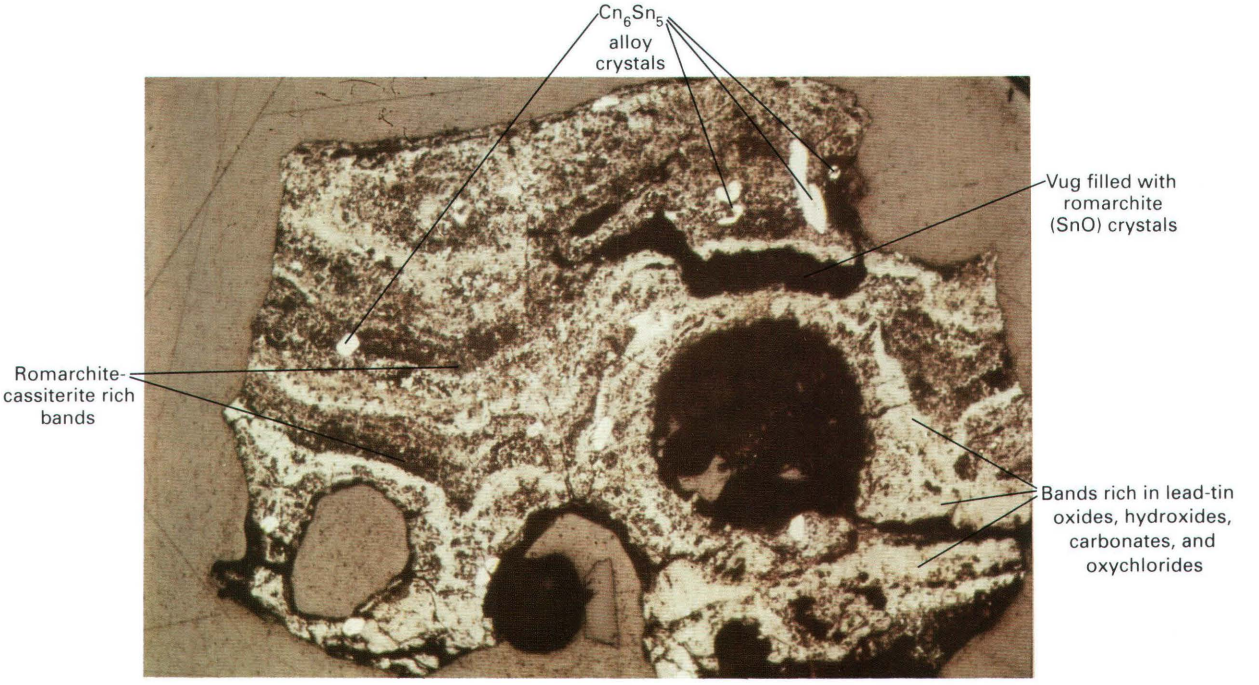

Figure 27. Photomicrograph of a nugget (sample Box 10D) from St. Croix showing several white euhedral crystals of Cu6Sn5 in a complex, layered matrix of romarchite-cassiterite (dark brown bands) and lead-tin oxides, hydroxides, carbonates, and oxychlorides (buff). The large oblong vug is filled with euhedral crystals of romarchite (SnO). Field of view = 2×1.5 mm.

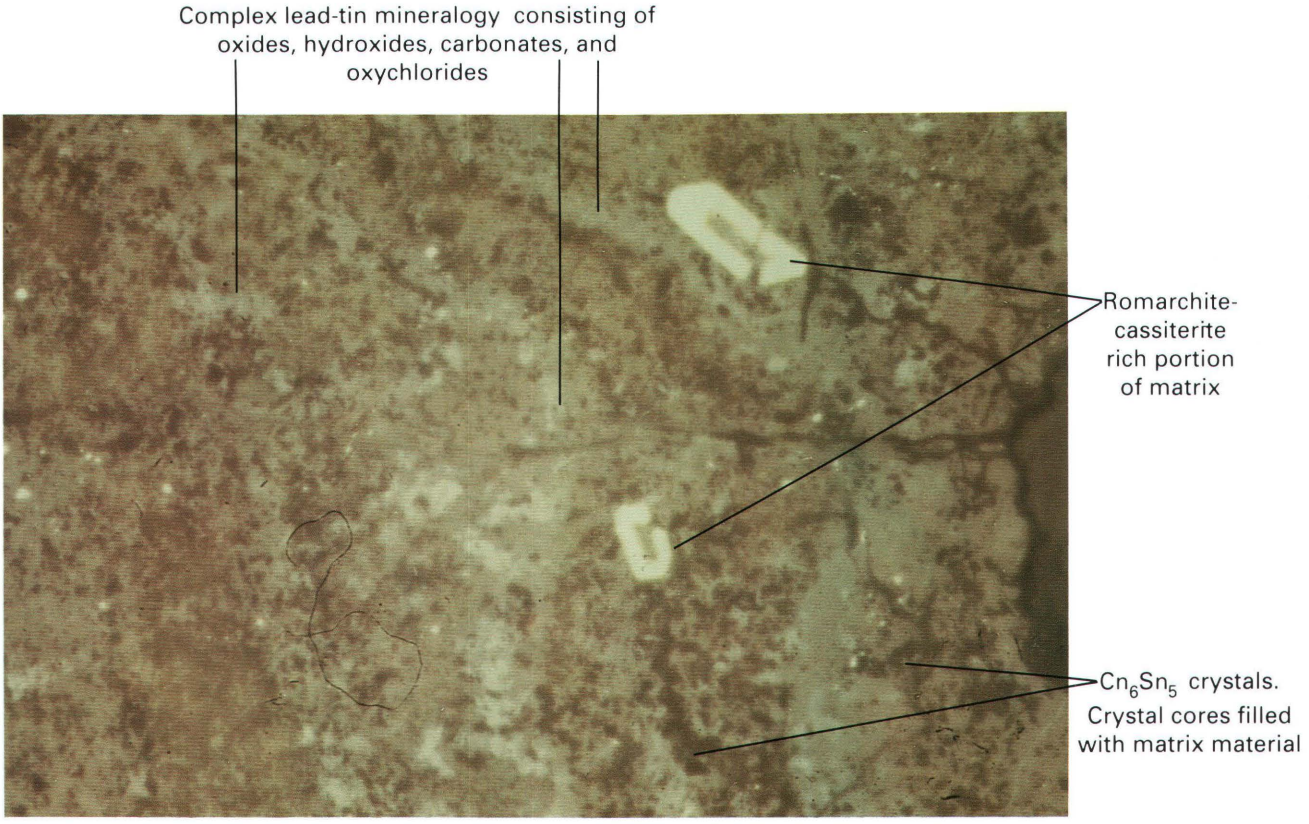

Figure 28. Photomicrograph showing a closeup of two of the Cu_6Sn_5 crystals (white) in the nugget (sample Box 10D) shown in figure 27. The crystals occur in a matrix (yellow) of cerussite, romarchite and lead-tin oxides, hydroxides, carbonates and oxychlorides. Field of view = 0.6 × 0.4 mm.

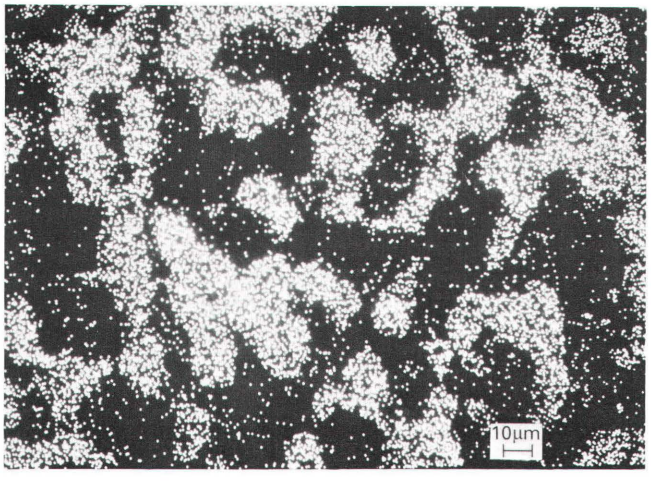

Figure 29. EDPM map of tin (light phase) in the eutectoid portion of the nugget (sample SC514) shown in figures 18 and 19. Scale bar = 5 µm.

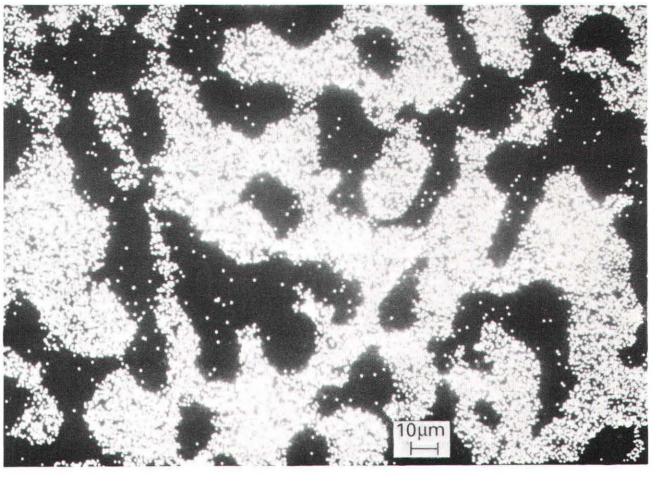

Figure 30. EDPM map of lead (light phase) in the eutectoid portion of nugget (sample SC514) shown in figures 18 and 19. Scale bar = 10 µm.

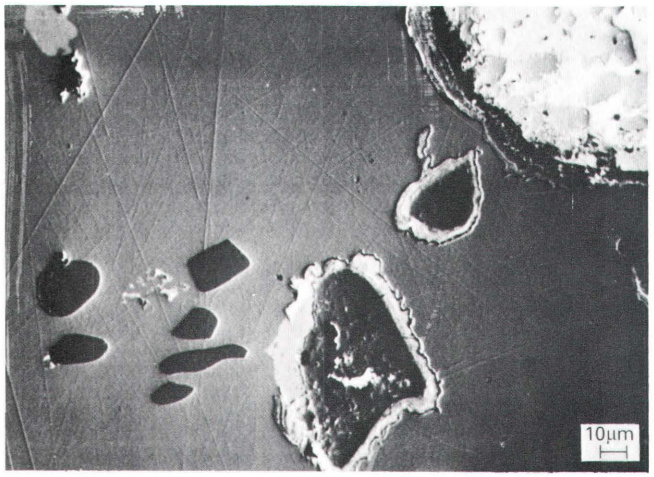

Figure 31. BES photomicrograph of a portion of a mineralogically complex copper nugget (sample SC514PA). A mineralogic map of this portion of the nugget is shown in figure 37; whereas, EDPM maps of individual elements, within this area, are shown in figures 32 through 36. Scale bar = 10 µm.

Figure 32. EDPM map of copper (light area) in a part of the nugget (sample SC514PA) shown in figure 31. Scale bar = 10 µm.

Figure 33. EDPM map of lead (light area) in the part of the nugget (sample SC514PA) shown in figure 31. Scale bar = 10 µm.

Figure 34. EDPM map of sulfur (light area) in the part of the nugget (sample SC514PA) shown in figure 31. Scale bar = 10 µm.

Energy dispersive spectrometry (EDS) analyses of numerous other samples of native lead and tin show that the individual metals are usually quite pure. Small bits of the harder tin are included within the mass of softer native lead because they were forced into the lead during sample preparation. In addition, alumina (Al_2O_3), also present within native lead as tiny specks, were probably emplaced during the final polishing. Microprobe analyses of the alumina contained within native lead in sample SJ601A and within cerussite in sample SJ105S are nearly identical to those for synthetic alumina.

Actual artifacts (piping and containers from 18th and 19th century stills, obtained from a local resident), consisting of elemental lead and tin plus lead, were examined. The lead portion of the two types of artifacts contains alumina spheres that are not found in the natural material. The alumina spheres are from the use of a gibbsite flux. In addition, the material from the artifacts typically contains 100 ppm or more silver while the natural material does not.

Nuggets and spheres of native copper are also relatively common. They are 0.5 to 1 mm across, or similar in size to the nuggets and masses of native tin-lead intergrowths. An example of these nuggets is shown in figures 31 to 37 (sample SC514PA). Copper nuggets and spheres are sometimes mineralogically complex, such as sample SC514PA, and then contain copper, zinc, and lead sulfides, copper-tin alloys, copper oxides, and other intergrown minerals.

Coatings of cotunnite, paratacamite, tenorite, cuprite, and other minerals are present on some spheres. Spheres of tenorite and cuprite, as much as 1 mm or more across, are presumably after native copper. A microprobe analysis of

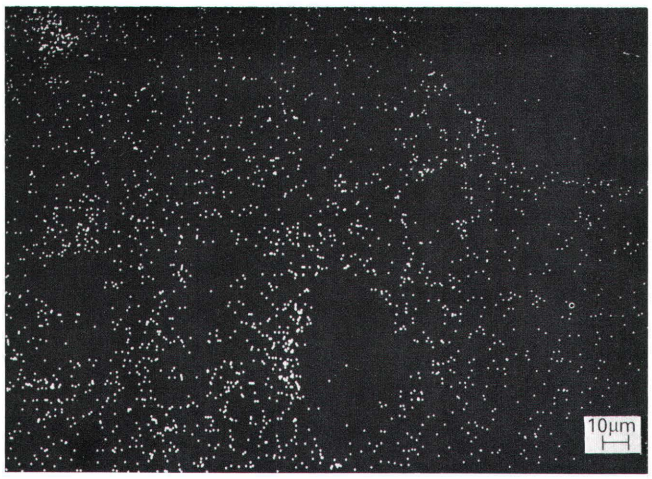

Figure 35. EDPM map of tin (light area) in the part of the nugget (sample SC514PA) shown in figure 31. Scale bar = 10 μm.

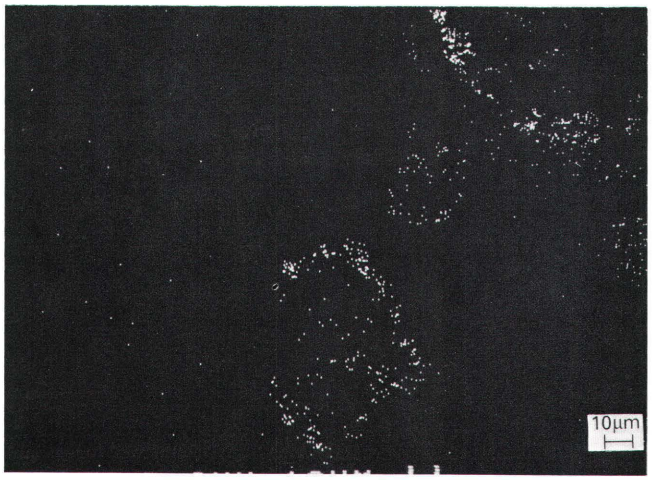

Figure 36. EDPM map of chlorine (light area) in the part of the nugget (sample SC514PA) shown in figure 31. Scale bar = 10 μm.

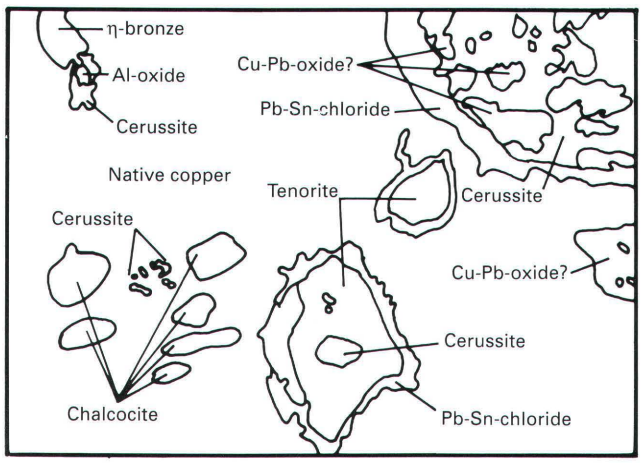

Figure 37. Mineral distribution map of the part of the nugget (sample SC514PA) shown in figure 31.

Table 7. Microprobe analyses of native copper, chalcocite, and cuprite grains in one nugget of native copper (sample SC514PA) from the U.S. Virgin Islands, in weight percent

Mineral	Native copper (Cu)	Chalcocite (Cu_2S)	Cuprite (CuO)
Number of analyses.....	11	2	1
Cu	90.4	79.4	79.2 (ideal 79.9)
Sn	8.4	0.0	0.1
Ni	0.3	---	---
Zn	0.5	0.0	0.0
S	--	20.2	0.0
Pb	0.0	0.1	0.0
Total	99.6	99.7	79.3

Table 8. Microprobe analyses of Cu_6Sn_5 (η-bronze) nuggets from three sample sites in the U.S. Virgin Islands, in weight percent

Sample.....	10C	10D	SJ738-2 Grain 16	Theoretical η -bronze
Number of analyses.....	9	3	3	
Sn	61.5	61.1	61.1	60.9
Ni	0.0	0.3	0.6	0.0
Cu	38.4	38.2	38.2	39.1
Total.....	99.9	99.6	99.9	100.0

native copper is given in table 7 showing a tin content much higher than that of associated chalcocite and cuprite.

Analysis of another sample of native copper in sample SC514I yielded (in wt. percent) copper 98.9, zinc 0.9, total=99.8. Tin, nickel, lead, sulfur, silicon, chlorine, and aluminum were looked for but were not detected.

Native gold and electrum are widespread throughout the U.S. Virgin Islands. Perhaps the best occurrence of native gold, along with associated Ag-Bi-Te mineralization, is in a 1 m thick quartz vein that strikes N. 70° W. and dips 15° N. on the south side of St. Thomas adjacent to Charlotte Amalie Harbor. Here, particles of gold as broad as 1 mm are in vuggy bull quartz. The grade of samples from this quartz vein ranged from 0.2 to 0.75 oz/ton gold. Alloys include electrum and Cu_6Sn_5 (η-bronze). This latter alloy has been found at Panasqueira, Portugal, in oxidized tin ores (Clark, 1972) and in gold-platinum group concentrates in southeast Borneo (Stumpfl and Clark, 1965). This alloy is widespread on all the Virgin Islands. Microprobe analyses are given in table 8 for material from three samples sites.

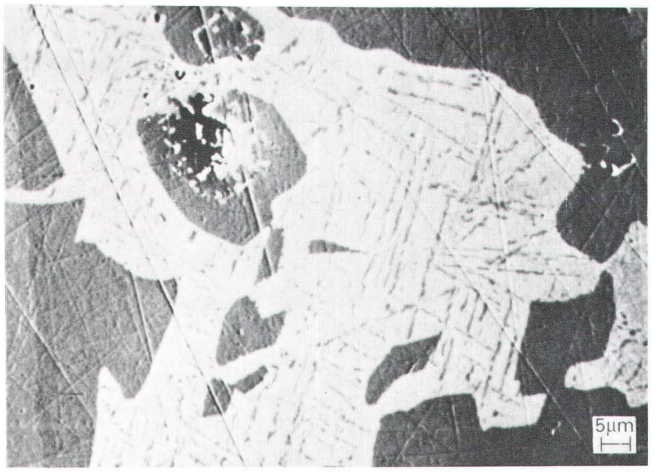

Figure 38. BSE photomicrograph of a portion of a copper nugget (sample SC514PA) showing nickel-bearing $Cu_{5.6}Sn$ alloy intergrown with native copper and associated chalcocite, sphalerite, and cotunnite. Scale bar = 5 μm.

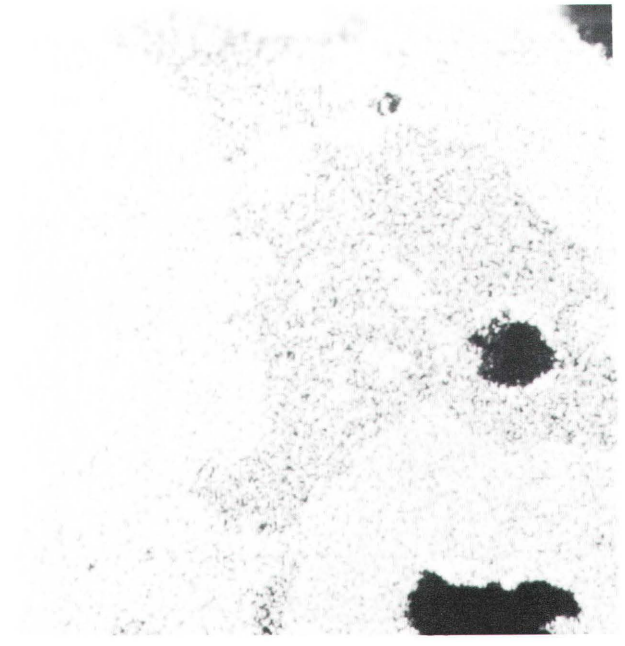

Figure 39. EDPM map of copper in the part of nugget (sample SC514PA) shown in figure 38. Scale bar = 5 μm.

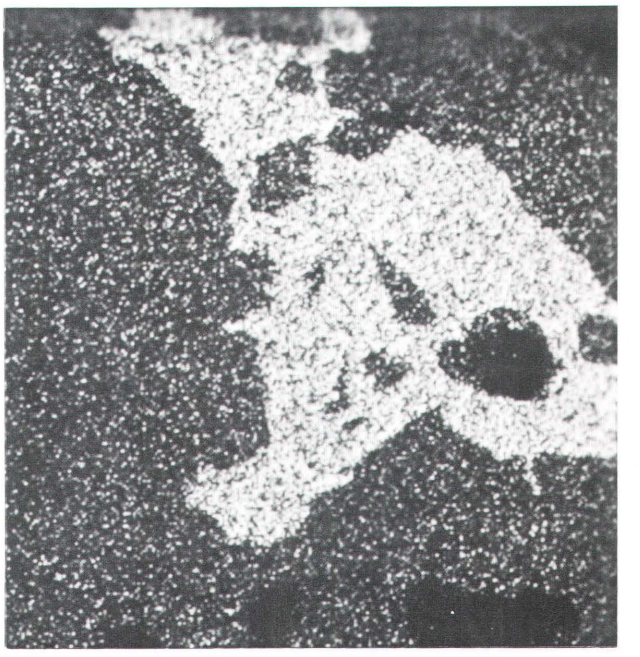

Figure 40. EDPM map of tin in the part of the nugget (sample SC514PA) shown in figure 38. Scale bar = 5 μm.

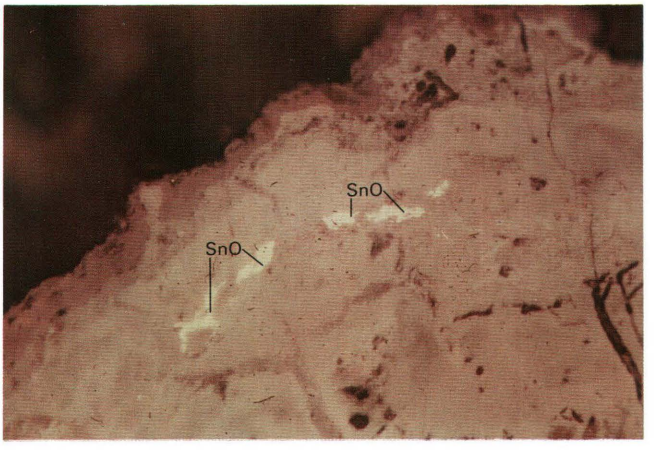

Figure 41. Photomicrograph showing anhedral, lenticular masses of white tin oxide (of the first type) within a magnetite-maghemite grain (cream-buff) from sample site 84SJ601 on St. John. Field of view = 0.3× 0.2 mm.

Individual crystals of the η-bronze are generally euhedral, and skeletal and range from 2–400 μm in maximum dimension. They are hosted by a mixture of fine-grained, white, lead-tin oxides, hydroxides, carbonates, and oxychlorides (fig. 27). Figure 28 shows two skeletal crystals in a matrix of cerussite, romarchite, and cassiterite. Both η-bronze and native tin can also occur together in a matrix of cerussite and other lead minerals. Confirmation of the η-bronze is afforded by X-ray diffraction data closely matching synthetic and natural material (Clark, 1972).

We also have found very sparse amounts of what appears to be Ni-bearing $Cu_{5.6}Sn$ intergrown with native copper (figs. 38–44), and associated with chalcocite, cotunnite, sphalerite, and other as yet unidentified minerals. The mineral is not homogeneous but shows an exsolution texture (fig. 38). Microprobe analyses of this phase are given in table 9. The analytical totals are approximately 6 weight percent low, and no other elements heavier than sodium were detected.

X-ray diffraction studies of this latter phase were not possible because of the exceedingly small grain size.

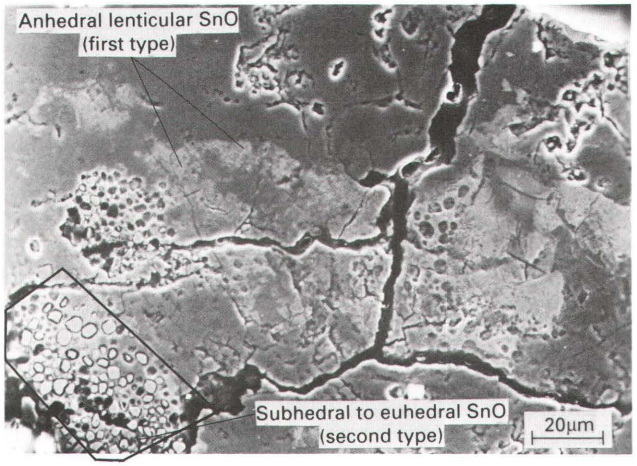

Figure 42. SEM photomicrograph of discrete segregations of subhedral to euhedral fine-grained tin oxide crystals in another grain of magnetite-maghemite from sample site 84SJ601 on St. John. An example of the first mode of occurrence of tin oxide can also be seen in this picture. Scale bar = 20 μm.

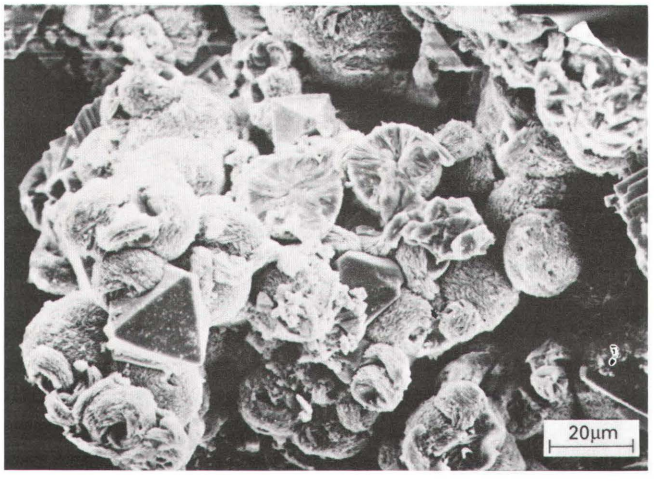

Figure 43. SEM photomicrograph of tin chloride-oxychloride (spherical) and tin-lead chloride and/or oxychloride (octahedral) filling a vug in a rock sample of the Caledonia Formation collected at sample site 84SC225 on St. Croix. Scale bar = 20 μm.

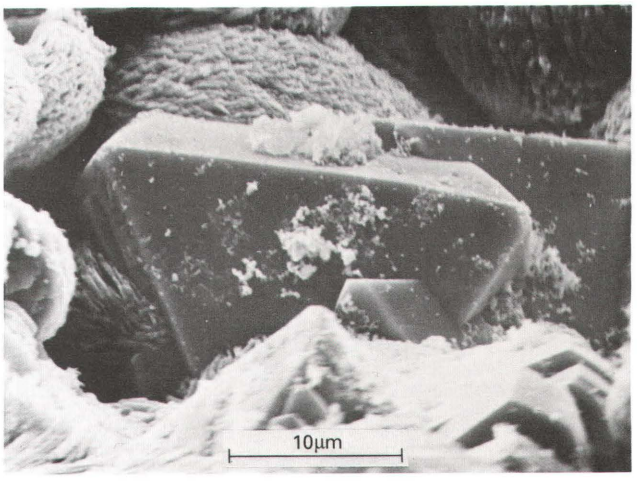

Figure 44. SEM photomicrograph showing a closeup of the tin-lead chloride and/or oxychloride occurring at sample site 84SC225. Scale bar = 10 μm.

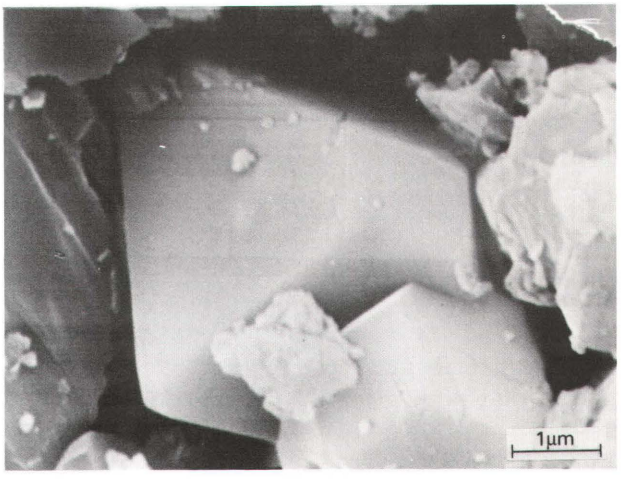

Figure 45. SEM photomicrograph of a romarchite (SnO) crystal in a rock sample collected at sample site 84SJ515 on St. Croix. Scale bar = 1 μm.

Various tellurides of gold and silver as well as bismuth have been identified by SEM methods. No X-ray diffraction studies of the tellurides were possible because of the small grain size.

Metallic oxides of tin, tin-lead, lead, lead-tin, copper, iron and chromium oxides have been identified (table 3). We wish to draw particular attention to the occurrence of black tin oxide—romarchite (SnO). Romarchite has been found on all the Virgin Islands, both in outcrop samples as well as in soil and stream-sediment concentrates. The only other reported occurrence of romarchite is as an alteration product, along with hydroromarchite, $Sn_3O_2(OH)_2$ (Howie and Moser, 1973), of tin pannikins that were immersed in fresh water (Organ and Mandarino, 1971). X-ray lines for romarchite from the U.S. Virgin Islands are shifted slightly to lower *d*-spacings reflecting the substitution of about 10–20 molecular percent isostructural PbO.

As can be seen in figures 9, 12, and 15, elevated concentrations of tin are commonly present in magnetic iron oxides on all three of the U.S. Virgin islands. On the basis of SEM EDS studies of grain mounts and polished sections of intergrown magnetite and maghemite grains variably altered to hydrous iron oxides (goethite and/or lepidocrocite), it appears that the tin is present as discrete inclusions of tin oxide as well as in limited solid solution in magnetite. Figure 41 shows discrete inclusions of tin oxide in a

Table 9. Microprobe analyses of of $Cu_{5.6}Sn(?)$ phase from copper nugget from sample site 84SC514PA from St. Croix, U.S. Virgin Islands, in weight percent

[Other elements looked for and not detected: S, Si, Cl, Zn, and Al. Electron dispersive spectrometry analysis shows minor Co to be present as well]

Type of material	Light-gray matrix	Dark exsolution laths
Number of analyses	8	3
Sn	24.1	20.6
Ni	1.6	1.2
Cu	67.5	72.3
Pb	0.3	0.2
Total	93.5	94.3

composite magnetite-maghemite grain. The tin oxide also occurs in the form of microveinlets that are tens of microns thick and as much as several millimeters in length within the mixed magnetite and maghemite grains. Figure 42 shows two modes of occurrence of tin oxide in the iron oxide grains. The first type (figs. 41 and 42) is represented by anhedral and lenticular masses of tin oxide. The second type (fig. 42) is represented by very discrete segregations of subhedral to euhedral fine-grained tin oxide crystals. The second type is nearly pure SnO_2; whereas, the first type contains appreciable iron. The small grain size precluded X-ray diffraction identification.

SEM-EDS studies also showed the occurrence of a discrete lead mineral within iron oxide grains collected at the same sites as the tin oxide-bearing ones. X-ray diffraction study data for the lead mineral could not be matched with any known compound. Emission spectrographic analysis of the hand-magnetic fraction indicate that the lead and tin occur together on all three islands. The sample shown in figures 41 and 42 (84SJ601) is characterized by a >2000 ppm tin content and 1000 ppm lead.

The regional correlation between the tin contents in the nonmagnetic fraction of heavy mineral concentrates (including native metals and halides), the tin contents in the hand-magnetic fraction (including cassiterite in magnetite/maghemite) and the precious metals in the whole rock, soil, and stream sediment samples provides conclusive evidence that the unusual tin and lead mineral assemblage is not of man-made origin.

HALIDES

Of particular interest and significance are the occurrences of halides and halogenides. Hosking (1970), described tin chloride and tin oxychloride alteration products from tin ingots in seawater. Abhurite, a tin hydroxychloride, was described by Matzko and others (1985). At least two new hydroxide chlorides or hydrated chlorides of tin and tin/lead have been found in the U.S. Virgin Islands. All these are white and are fine-grained. A nugget of native tin-lead contains a cavity filled with two tin oxychloride or hydroxychloride minerals. Figures 43 to 45 show the morphology of some of these tin-lead minerals. These compare very well with some of the phases grown in the synthetic experiments (figs. 46*A*–46*F*). X-ray diffraction data were obtained on both natural and synthetic materials, but the intimate admixture of the various hydrated tin-lead oxides, hydroxides, oxychlorides, and other compounds prevented discrimination of individual minerals. Attempts were made to match diffraction data with known compounds; except for the minerals named in this section, matches were not found. One or more iron chloride minerals are present as well. Other rare chlorides of lead, copper, and bismuth, as well as cerargyrite, iodargyrite, and bromargyrite have also been identified.

SULFIDES

Sulfides are present as well, even though this area has deep tropical weathering that is not conducive to the survival of sulfides in the surface or near-surface environment. The mineralogy is simple for the most part, and drill hole cuttings or core would undoubtedly reveal the presence of additional species. Pyrite, galena, sphalerite, chalcocite, and acanthite predominate (table 3). A Ni-As-S mineral was identified by SEM EDS, and may be gersdorffite (NiAsS). This has not been confirmed by X-diffraction). A tin sulfide is present but the specific mineral or minerals have not yet been determined.

SULFATES, PHOSPHATES, AND CARBONATES

Several different sulfates, phosphates, and carbonates have been identified as well as one vanadate, probably mottramite. The most common species are barite, cerussite, and hydrocerussite. Hydrocerussite is relatively common along with cerussite. Cerussite is distinctive because of its blue luminescence under the electron beam.

An induction coupled plasma–atomic emission spectroscopic (ICP–AES) analysis of blue-green turquoise from the White Cliffs on St. John showed: 14.4% Al, 7.8% Fe, 0.19% Na, 14.2% P, 4500 ppm As, 260 ppm Ba, 220 ppm Bi, 5.7% Cu, 100 ppm Ga, 1000 ppm Sc, and 7300 ppm Zn. This material is best characterized as a ferrian turquoise. X-ray diffraction studies confirmed the mineral to be turquoise.

SILICATES

Much more work needs to be done on the various silicates. The minerals listed in table 3 are those occurring in mineralized areas in addition to quartz, feldspars, and other rock-forming silicates. An occurrence of wairakite from St. Thomas was described by Donnelly (1962).

This unique mineral assemblage points toward an unusual mineralization system. While we know a fair amount about the mineralogy and geochemistry of high-temperature tin deposits and occurrences, our knowledge of low-temperature tin minerals and their geochemistry is woefully lacking.

LABORATORY CRYSTAL SYNTHESIS

A series of laboratory crystal synthesis experiments were conducted at room temperature and one atmosphere pressure in an attempt to replicate the formation of lead and tin chlorides and oxychlorides in an environment similar to that postulated to have existed within the St. Croix graben during mineral formation. Dilute solutions of tin and lead chlorides were injected into a sea-water saturated $CaCO_3$ slurry at a slow rate. Subsequent to the exhaustion of the chloride reservoirs, the slurry was permitted to evaporate to dryness, and the resultant material was inspected using the SEM and X-ray diffraction techniques. Chlorides/oxychlorides of tin (fig. 46*A*), lead (fig. 46*B*), tin-lead (fig. 46*C*) and romarchite (fig. 46*D*) were identified. These synthetic minerals were compositionally and morphologically identical to those found in the U.S. Virgin Islands. It is believed, but could not be verified, that native tin was also present. Experiments using lower pH values produced coarse romarchite (fig. 46*E*) and abundant native tin (fig. 46*F*).

DISCUSSION

The precious- and base-metal anomalies found on the U.S. Virgin Islands cross nearly all the rock types exposed on the islands, including the Kingshill Marl of mid to late Miocene age on St. Croix (Lidz, 1988). A good spatial correlation between the geochemical patterns and major mapped structural features can be seen on all three islands, but they are especially clear on St. Croix and St. John. Hydrothermal alteration (predominantly silicification and sericitization) is widespread and is especially visible along the southern shores of St. John and St. Thomas. The alteration occurring in the interior parts of the islands tends to be masked by the pervasive and deep weathering and can only be seen in road cuts or at construction sites. Pyritization was widespread on the islands but fresh pyrite can only be found encapsulated in the more siliceous rock units. Other sulfides are rare, although a little galena, chalcopyrite, and sphalerite have been found in the heavy-mineral concentrates and rock samples. Epidotization on the islands was widespread and sometimes massive. Barite and gossan fragments are common in heavy-mineral concentrates.

Gossan is present at several locations on the islands. The most massive gossan caps Bordeaux Mountain on St. John and is greater than 7 m in thickness. A thin gossan is also present on Cocoloba Point and a thin siliceous gossan caps the paratacamite coated White Cliffs (St. John), which consist of fine-grained hydrothermal quartz with thin turquoise veinlets.

A precious-metals bearing skarn, characterized by marble, garnetiferous rocks, and iron-bearing, as well as copper-bearing, quartz and barite veins, occurs on the islands to the north of and between St. Thomas and St. John, extending eastward to Mary Point on St. John.

Gossan and/or massive limonitic boxwork also occurs on St. Thomas, especially in the Jersey Bay area. No gossan has been noted on St. Croix although gossan fragments as well as epidote and barite, are widespread in the concentrates of soil and stream sediments.

Water-soluble chlorine in the soils of the islands consistently delineates halos over and around the base- and precious-metals anomalies. These chlorine-enriched areas do not show any correlation with nearness to shore-line, prevailing wind direction, or the highest areas on these islands.

The highly unusual halide and native metal rich base-metal mineralogy found in the surficial materials as well as outcrops and the predominance of silver halides points to a genetic sequence that involves an extremely chlorine-rich solution phase. This conclusion is also supported by the survival of the tin and lead chlorides/oxychlorides only in settings of encapsulation, whether these be within native-metal grains or within outcrops of dense, siliceous units.

At this stage of the study, the U.S. Virgin Island geochemical anomalies indicate a mineralization that is a distinct and unique mineral occurrence. The current erosional level intersects this mineralization system at its upper levels. It is postulated that this mineralization is probably related to subcropping felsic to intermediate intrusives of late Tertiary age. The metal-rich hydrothermal solutions were probably introduced into shallow, calcareous, ooze-rich, semi-restricted sea basins—as exemplified by the central St. Croix graben (fig. 47). Here, the graben boundary faults acted as the main hydrothermal solution pathways. Within the graben the more porous terrigenous alluvium zone, near the graben walls, would facilitate the further migration of these fluids and their gradual dissemination into the graben water. The immediate area of the graben was probably additionally enriched in sodium chloride as a result of sea water convection currents due to the thermal gradient resulting from the introduction of the warm hydrothermal solutions. Higher rates of evaporation might result within the shallow part of the graben as a result of the thermal gradient brought about by the introduction of the warm hydrothermal

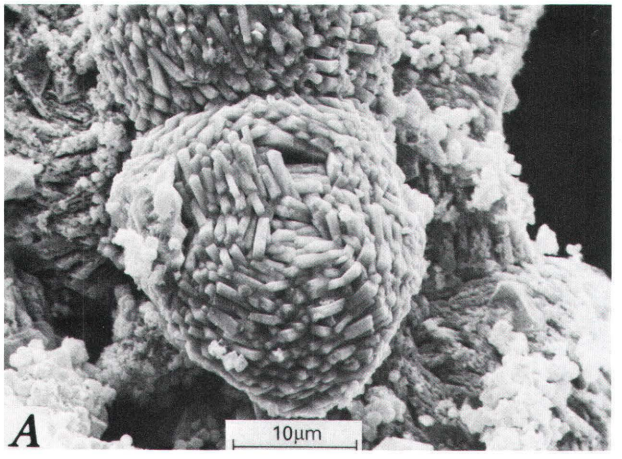

A. Spherical tin chloride-oxychloride.

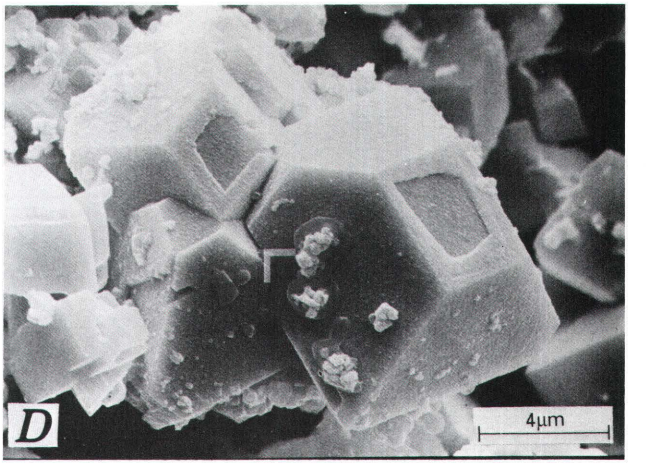

D. Octahedral crystals of romarchite (SnO).

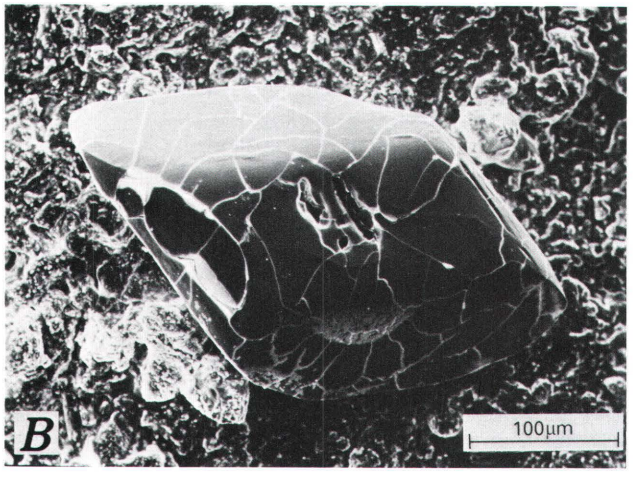

B. Large crystal of lead chloride-oxychloride.

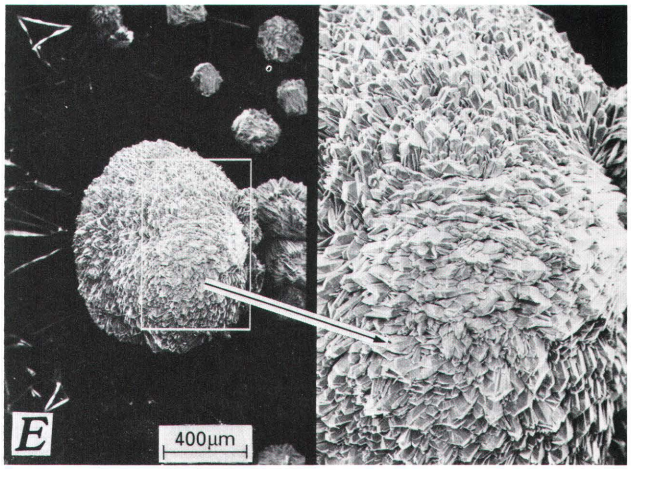

E. Spherical romarchite (SnO) with enlargement to show individual crystals on the left.

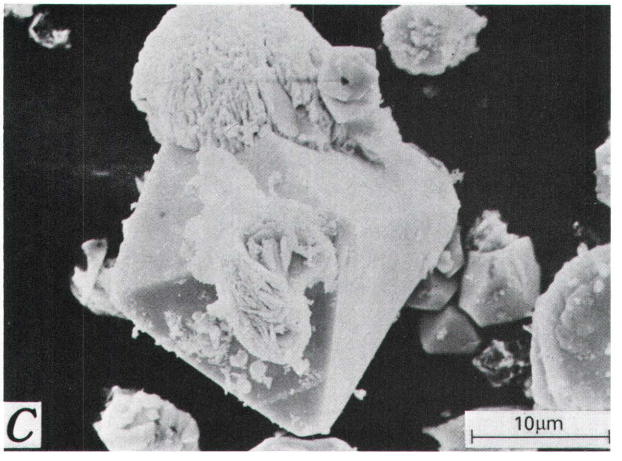

C. Octahedral crystal of tin-lead chloride-oxychloride.

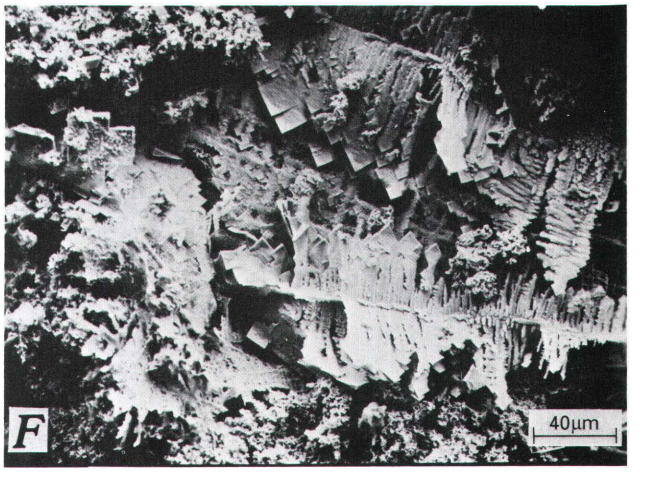

F. Feathery, skeletal crystal of native tin.

FIGURE 46. SYNTHETIC MINERALS GROWN AT ROOM TEMPERATURE AND ONE ATMOSPHERE PRESSURE BY INJECTING CHLORIDES OF LEAD AND TIN INTO SEA WATER-SATURATED, POWDERED $CaCO_3$.
[Shown at different scales.]

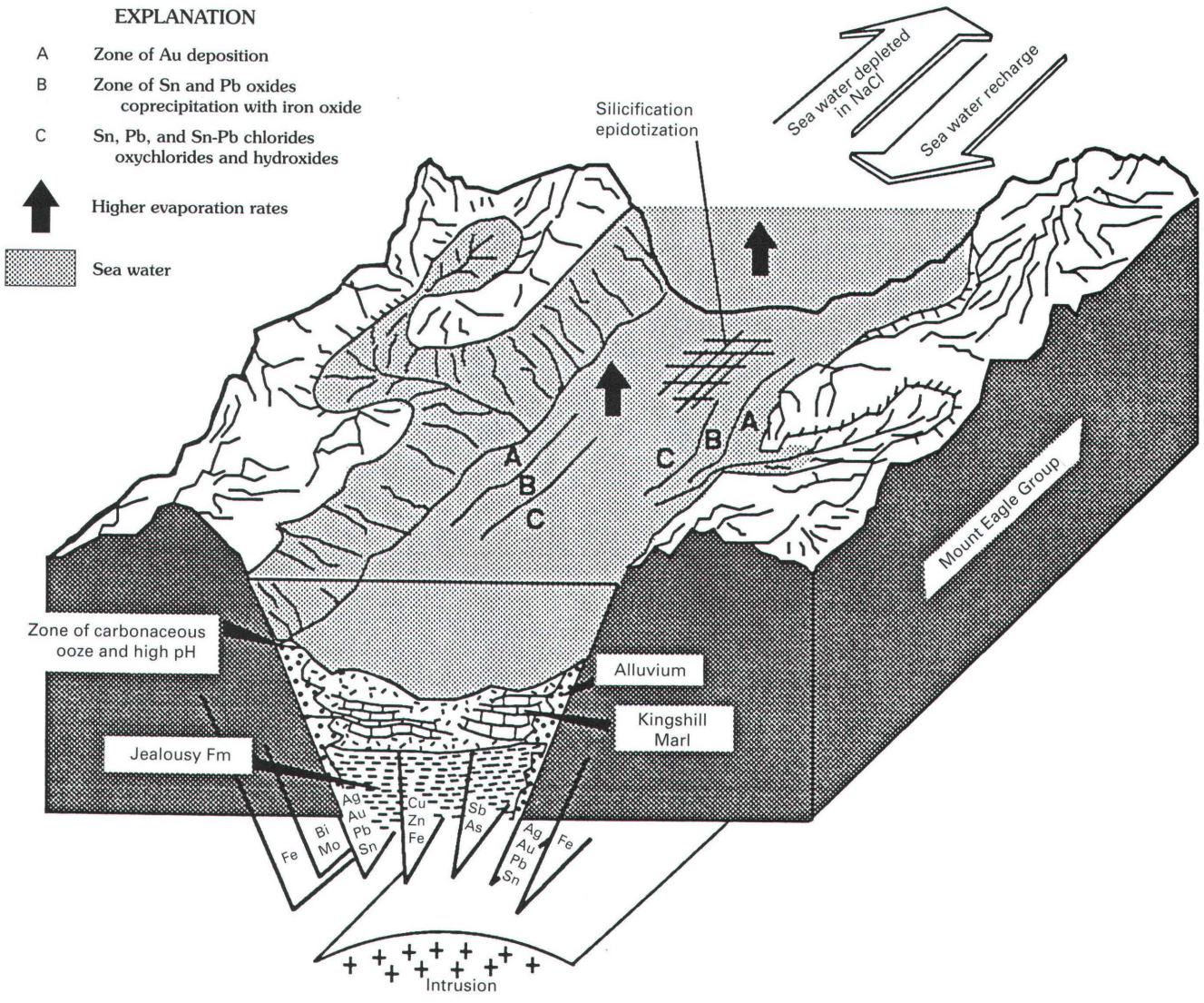

Figure 47. Block diagram illustrating the conceptual model of precious- and base-metal mineralization in the St. Croix graben, U.S. Virgin Islands.

solutions as well as the relatively shallow water setting here. It is probable that the introduced metals were deposited primarily as halides. All evidence indicates the presence of hydrothermal solutions that were tungsten, fluorine, and sulfur poor but which were very rich in chlorine. Paucity of sulfur is indicated by the nearly total absence of nearly all base-metal sulfides—aside from pyrite, which is not part of this mineralization. In addition to occuring within the halides, oxides, and carbonates, the base-metals here also occur built into the layered magnetite/maghemite layers in substantial concentrations primarily adjacent to the eastern and western graben walls. A zonational aspect is evident relative to the graben walls: gold is concentrated in the immediate vicinity of the walls and of cross-trending structures; whereas, silver and base-metals are zoned outward from the graben boundary faults. The graben-filling Kingshill Limestone (or marl) has been silicified and epidotized to varying degrees and base-metal chlorides have been found cementing fragments of biota within the marl, but more commonly the base-metal chlorides occur within the grains of native tin and lead that are nearly ubiquitous in the soils within the graben. Gold is widespread near the graben walls generally in the form of submicron particles although some coarser particles of gold have been found in sediments from the most strongly silicified and epidotized portions for the graben.

Simple laboratory syntheses, at room temperature and one atmosphere pressure, produced tin and lead and tin-lead chlorides, that are compositionally and morphologically identical to those found on the U.S. Virgin Islands. Romarchite and some possible native tin were also produced. Increasing the pH of the solution produced coarse, well-crystallized romarchite and abundant native tin.

Recent unpublished work by the authors has indicated that lead, tin, iron, magnesium, and other chlorides, oxychlorides, carbonates, hydroxides, and other compounds are associated with base- and precious-metal mineralization in the Bayhorse area in Idaho as well as the Duluth Complex and the granite-greenstone terrain in northeastern Minnesota. Total chlorine, determined using stream-sediment samples, form halos that are associated with most of the examined mineralized areas in Idaho.

SUMMARY

This geochemical study of the U.S. Virgin Islands demonstrates the presence of an extensive tin-lead and precious-metals metallogenic province in the northeastern portion of the Greater Antilles island arc. The U.S. Virgin Islands hydrothermal systems are characterized by a near absence of tungsten, fluorine, and sulfur and a superabundance of chlorine. The abundance of chlorine is probably due, at least in part, to the submarine origin of this mineralization. These conditions produced a highly unusual base-metals mineralogy consisting, primarily of halides, complex halide-native metal intergrowths, and native metals.

The authors believe that the currently available data on the U.S. Virgin Islands demonstrates this area to be one worthy of further study for economic as well as scientific reasons.

REFERENCES

Abbey, S., 1980, Studies in "standard samples" for use in the general analysis of silicate rocks and minerals: Geological Survey of Canada, Paper 80–14, 30 p.

Alminas, H.V., and Mosier, E.L., 1976, Oxalic-acid leaching of rock, soil, and stream-sediment samples as an anomaly-accentuation technique: U.S. Geological Survey Open-File Report 76–275, 24 p.

Aleksandrov, A.I., 1955, Native tin in alluvial placers of the river Is (Central Urals): Zapiski Vsesoyuznogo Mineralogicheskogo Obshchestvo, 84, p. 462–464. [In Russian]

Clark, A.H., 1972, A copper-tin alloy (ηCu_6Sn_5) from Panasqueira, Portugal: Neues Jahrbuch für Mineralogie Monatshefte p. 108–111.

Cleve, P.T., 1881, Outline of the geology of the northeastern West India Islands: Annals of the New York Academy of Sciences, v. 2, p. 185–192.

Cox, D.P., Marvin, R.F., McGonigle, J.W., McIntyre, D.H., and Rogers, C.L., 1977, Potassium-argon geochronology of some metamorphic, igneous, and hydrothermal events in Puerto Rico and the Virgin Islands: Journal of Research, U.S. Geological Survey, v. 5, p. 689–703.

Donnelly, T.W., 1959, Geology of St. Thomas and St. John, Virgin Islands: Princeton University, Ph. D. thesis, 191 p.

———1962, Wairakite in West Indian spilitic rocks: American Mineralogist, 47, p. 794–802.

——— 1966, Geology of St. Thomas and St. John, U.S. Virgin Islands: Geological Society of America Memoir 98, p. 85–176.

Earle, K.W., 1924, The geology of the British Virgin Islands: Geology Magazine, v. 61, p. 339–351.

Filimonova, L.G., Gorshkov, A.I., Korina, Ye. A., and Trubkin, N.V., 1981, Native metals in volcanic rocks of the southern Sikhote Alin: Doklady Akademii Nauk SSSR, 256, no. 4, p. 962–965. [In Russian]

Foord, E.E., Alminas, H.V., and Tucker, R.E., 1988, Tin, gold, and base-metal mineralization in the U.S. Virgin Islands: Abstract V. M. Goldschmidt Conference, May 11–13, 1988, Baltimore, Maryland, p. 41–42.

Gill, I.P., 1990, The evolution of Tertiary St. Croix: Applied Carbonate Research Program, Technical Series; Contribution no. 58, 287 p.

Grimes, D.J., and Marranzino, A.P., 1968, Direct-current arc alternating-current spark emission spectrographic field methods for the semiquantitative analysis of geologic materials: U.S. Geological Survey Circular 591, 6 p.

Helsley, C.E., 1960, Geology of the British Virgin Islands: New Jersey, Princeton University, Ph. D. thesis, 219 p.

Hopkins, R.T., Tucker, R.E., Roemer, T.A., Sharkey, J.D., and Alminas, H.V., 1986, Analytical results from a geochemical survey of the U.S. Virgin Islands: U.S. Geological Survey Open-File Report 86–86, 229 p.

Hosking, K.F.G., 1970, Chloride and oxychloride of tin on old ingots: Geological Society of Malaysia Newsletter, no. 27, p. 5–7.

———1974, The native tin story, Geological Society of Malaysia Newsletter, no. 50, p. 6–11.

Howie, R.A., and Moser, W., 1973, Crystal data and formula for hydrous tin(II) oxide: a note: American Mineralogist, 58, p. 552.

Kesler, S.E., and Sutter, J.F., 1979, Compositional evolution of intrusive rocks in the eastern Greater Antilles Island arc: Geology, v. 7, p. 197–200.

Krylova, V.V., 1975, First find of native lead in a gold-silver deposit in the northeastern USSR: Doklady Akademii Nauk SSSR, 221, no. 2, p. 445–446. [In Russian]

Kucha, Hans, 1981, Precious metal alloys and organic matter in the Zechstein copper deposits, Poland: Tschermaks Mineralogische Petrographische Mitteilungen 28, p. 1–16.

Lawrence, L.J., 1951, Notes on an occurrence of native tin at Emmaville, N.S.W.: The Australian Journal of Science, v. 13, no. 1, p. 82–84.

Lidz, B.H., 1988, Upper Cretaceous (Campanian) and Cenozoic stratigraphic sequence, northeast Caribbean (St. Croix, U.S. Virgin Islands): Geological Society of America Bulletin, v. 100, p. 282–298.

Matzko, J J., Evans, H.T., Jr., Mrose, M.E., and Aruscavage, P., 1985, Abhurite, a new tin hydroxychloride mineral, and a comparative study with a synthetic basic tin chloride: Canadian Mineralogist, v. 23, p. 233–240.

McHugh, J.B., Tucker, R.E., Hopkins, R.T., Roemer, T.A., and Alminas, H.V., 1989, Gold, silver, tellurium, and spectrographic analyses for rock and soil samples from the U.S. Virgin

Islands: U.S. Geological Survey Open-File Report 89–355, 64 p.

Meyerhoff, H.A., 1926, Scientific survey of Puerto Rico and the Virgin Islands: New York Academy of Sciences, v. 14, parts 1–2, p. 71–219.

Meier, A.L., 1980, Flameless atomic absorption determination of gold in geological materials: Journal of Geochemical Exploration, v. 13, p. 77–85.

Novgorodova, M.I., Gorshkov, A.I., Trubkin, N.V., Veretnikov, V.M, and Tsepin, A.I., 1981, An exotic mineral association with uraninite: Mineralogicheskii Zhurnal, v. 3, p. 102–108. [In Russian].

Okrugin, A.V., Oleinikov, B.V., Zayakina, N.V., and Leskova, N.V., 1981, Native metals in trap rocks of the Siberian Platform: Zapiski Vsesoyuznogo Mineralogicheskogo Obshchestvo, v. 110, p. 186–204. [In Russian]

Organ, R.M., and Mandarino, J.A., 1971, Romarchite and hydromarchite, two new stannous minerals: Canadian Mineralogist, v. 10, p. 916.

Schell, B.A., and Tarr, A.C., 1978, Plate tectonics of the Northeastern Caribbean Sea region: Geologie En Mijnboow, v. 57(2), p. 319–324.

Silman, J.F.B., 1954, Native tin associated with pitchblende at Nesbitt LaBine Uranium mines, Beaverlodge, Saskatchewan: American Mineralogist, v. 39, p. 529–530.

Stumpfl, E.F., and Clark, A.M., 1965, Electron-probe microanalysis of gold-platinoid concentrates from southeast Borneo: Transactions of the Institute of Mining and Metallurgy, v. 74, p. 933–946.

Taggart, J.E., Jr., Lindsay, J.R., Scott, B.A., Vivit, D.V., Bartel, A.J., and Stewart, K.C., 1987, Analysis of geological materials by wavelength-dispersive X-ray fluorescence spectrometry, *in* Baedeker, P.A., editor, Methods for geochemical analysis: U.S. Geological Survey Bulletin 1770, p. E7–E19.

Thompson, C.E., Nakagawa, H.M., and Van Sickle, G.H., 1968, Rapid analysis for gold in geologic materials: U.S. Geological Survey Professional Paper 600–B, p. 130–132.

Tomson, I.N., Polyakova, O.P., and Polokov, V.P., 1989, Graphite-ilmenite mineralization in tin deposits—An indicator of mantle gas jets (Primorye Region, USSR): Global Tectonics and Metallogeny, v. 3, p. 101–106.

Tucker, R.E., 1987, A geochemical study of St. John, U.S. Virgin Islands: Colorado School of Mines, Ph. D. thesis, 404 p.

Turovsky, S. D., 1956, The discovery of native tin in the northern Kirgizia: Trudy Institut Geologii, Kirgizia Filiala Akademii Nauk SSSR, no. 8, p. 125–129. [In Russian]

Uwadiale, G.G.O.O., and Hall, A.J., 1984, Tin mineralization in Agbaja sedimentary iron ore, Nigeria: Applied Earth Science, Institute of Mining and Metallurgy, Transactions, Section B, p. 87–89.

VanTrump, George, Jr., and Alminas, H.V., 1978, REM (relative element magnitude) Program Explanation and Computer Program Listing:U.S. Geologic Survey Open-File Report 78-1014, 18 p.

Whetten, J.J., 1962, Geology of St. Croix, U.S. Virgin Islands: New Jersy, Princeton University, Ph. D. Thesis, 102 p.

———1966, Geology of St. Croix, U.S. Virgin Islands: Geological Society of America Memoir 98, p. 177–239.

Manuscript approved for publication January 29, 1993
Graphics by Roger Highland
Edited by Thomas Kohnen
Photocompositon by Shelly A. Fields

☆ U.S. GOVERNMENT PRINTING OFFICE: 1994-673-046/86059

SELECTED SERIES OF U.S. GEOLOGICAL SURVEY PUBLICATIONS

Periodicals

Earthquakes & Volcanoes (issued bimonthly).
Preliminary Determination of Epicenters (issued monthly).

Technical Books and Reports

Professional Papers are mainly comprehensive scientific reports of wide and lasting interest and importance to professional scientists and engineers. Included are reports on the results of resource studies and of topographic, hydrologic, and geologic investigations. They also include collections of related papers addressing different aspects of a single scientific topic.

Bulletins contain significant data and interpretations that are of lasting scientific interest but are generally more limited in scope or geographic coverage than Professional Papers. They include the results of resource studies and of geologic and topographic investigations; as well as collections of short papers related to a specific topic.

Water-Supply Papers are comprehensive reports that present significant interpretive results of hydrologic investigations of wide interest to professional geologists, hydrologists, and engineers. The series covers investigations in all phases of hydrology, including hydrology, availability of water, quality of water, and use of water.

Circulars present administrative information or important scientific information of wide popular interest in a format designed for distribution at no cost to the public. Information is usually of short-term interest.

Water-Resources Investigations Reports are papers of an interpretive nature made available to the public outside the formal USGS publications series. Copies are reproduced on request unlike formal USGS publications, and they are also available for public inspection at depositories indicated in USGS catalogs.

Open-File Reports include unpublished manuscript reports, maps, and other material that are made available for public consultation at depositories. They are a nonpermanent form of publication that may be cited in other publications as sources of information.

Maps

Geologic Quadrangle Maps are multicolor geologic maps on topographic bases in 7 1/2- or 15-minute quadrangle formats (scales mainly 1:24,000 or 1:62,500) showing bedrock, surficial, or engineering geology. Maps generally include brief texts; some maps include structure and columnar sections only.

Geophysical Investigations Maps are on topographic or planimetric bases at various scales, they show results of surveys using geophysical techniques, such as gravity, magnetic, seismic, or radioactivity, which reflect subsurface structures that are of economic or geologic significance. Many maps include correlations with the geology.

Miscellaneous Investigations Series Maps are on planimetric or topographic bases of regular and irregular areas at various scales; they present a wide variety of format and subject matter. The series also includes 7 1/2-minute quadrangle photogeologic maps on planimetric bases which show geology as interpreted from aerial photographs. The series also includes maps of Mars and the Moon.

Coal Investigations Maps are geologic maps on topographic or planimetric bases at various scales showing bedrock or surficial geology, stratigraphy, and structural relations in certain coal-resource areas.

Oil and Gas Investigations Charts show stratigraphic information for certain oil and gas fields and other areas having petroleum potential.

Miscellaneous Field Studies Maps are multicolor or black-and-white maps on topographic or planimetric bases on quadrangle or irregular areas at various scales. Pre-1971 maps show bedrock geology in relation to specific mining or mineral-deposit problems; post-1971 maps are primarily black-and-white maps on various subjects such as environmental studies or wilderness mineral investigations.

Hydrologic Investigations Atlases are multicolored or black-and-white maps on topographic or planimetric bases presenting a wide range of geohydrologic data of both regular and irregular areas; the principal scale is 1:24,000, and regional studies are at 1:250,000 scale or smaller.

Catalogs

Permanent catalogs, as well as some others, giving comprehensive listings of U.S. Geological Survey publications are available under the conditions indicated below from USGS Map Distribution, Box 25286, Building 810, Denver Federal Center, Denver, CO 80225. (See latest Price and Availability List.)

"Publications of the Geological Survey, 1879-1961" may be purchased by mail and over the counter in paperback book form and as a set microfiche.

"Publications of the Geological Survey, 1962-1970" may be purchased by mail and over the counter in paperback book form and as a set of microfiche.

"Publications of the U.S. Geological Survey, 1971-1981" may be purchased by mail and over the counter in paperback book form (two volumes, publications listing and index) and as a set of microfiche.

Supplements for 1982, 1983, 1984, 1985, 1986, and for subsequent years since the last permanent catalog may be purchased by mail and over the counter in paperback book form.

State catalogs, "List of U.S. Geological Survey Geologic and Water-Supply Reports and Maps For (State)," may be purchased by mail and over the counter in paperback booklet form only.

"Price and Availability List of U.S. Geological Survey Publications," issued annually, is available free of charge in paperback booklet form only.

Selected copies of a monthly catalog "New Publications of the U.S. Geological Survey" is available free of charge by mail or may be obtained over the counter in paperback booklet form only. Those wishing a free subscription to the monthly catalog "New Publications of the U.S. Geological Survey" should write to the U.S. Geological Survey, 582 National Center, Reston, VA 22092.

Note.–Prices of Government publications listed in older catalogs, announcements, and publications may be incorrect. Therefore, the prices charged may differ from the prices in catalogs, announcements, and publications.